

**The impact of the vortex relocation scheme on hurricane initialization:  
Hurricane Joaquin (2015) as an example**

Chu-Chun Chang

Department of Atmospheric and Oceanic Science, University of Maryland College Park,

Maryland

Advisor Dr. Daryl T. Kleist and Dr. Kayo Ide

A scholarly paper in partial fulfillment of the requirements for the degree of

Masters of Science

December 2018

## **Acknowledgements**

The completion of the scholar paper is attributed to many peoples support and encouragement. First, I would like to gratefully and sincerely thank to my two advisors, Dr. Kayo Ide and Dr. Daryl Kleist, whose patient guidance and valuable suggestions make me successfully complete this scholar paper. I am also grateful to my officemates and students in UMD Chaos group, Cheng Da, Ni Dai, Takuma Yoshida, Tse-Chun Chen, Kriti Bhargava, and Luyu Sun, who has given me a lot of help in my work and emotional support in the daily life. I thank to Tse-Chun and Kriti for helping me set up the GDAS/GFS system on S4. I am grateful to Cheng and Takuma for a lot of insightful discussions. My special thanks also go to William Miller and Cheng Da for reviewing the draft and providing me invaluable suggestions to refine this paper.

Last but not the least, I would like to express my special thanks to my beloved mother and brother, who always encourage me and share their worries and happiness with me.

# Table of Contents

Acknowledgements .....	1
Table of Contents .....	2
Abstract.....	3
List of Figures.....	5
List of Tables.....	9
List of Abbreviations.....	10
1. Introduction.....	11
1.1 Previous studies on hurricane initialization .....	11
1.2 Motivation.....	16
2. The Impact of Different Data Assimilation Schemes on Hurricane Joaquin (2015) Case .....	18
2.1 Model and Data .....	18
2.2 Deterministic and Ensemble 5-day forecasts of the Regional Model .....	19
2.3 Impact of parameterization schemes on Joaquin prediction .....	23
2.4 The Impact of Regional Data Assimilation on Hurricane Joaquin (2015) .....	25
2.4.1 The Data Assimilation System and Experiment Setup .....	25
2.4.2 Real Case Experiments with WRF model: Joaquin (2015) case.....	26
3. The Impact of the Relocation Scheme on the GFS/GDAS system.....	30
3.1 Experimental Setup .....	30
3.2 Result comparison of Operational and the DA experiments .....	32
3.2 Impact of relocation on GDAS analysis .....	36
3.3 Impact of the relocation on the GFS forecast.....	52
4. Conclusion .....	55
4.1 Summary of Research.....	55
4.2 Future Direction .....	57
4.3 Acknowledgements.....	58
Reference .....	59

## **Abstract**

Hurricane initialization is an essential technique in numerical weather prediction. For the operational National Center for Environmental Prediction (NCEP) Global Forecast System (GFS), the hurricane initialization involves procedures of vortex bogusing, advisory minimum sea-level pressure assimilation, and hurricane relocation (Liu et al. 2000). The relocation scheme aims to reduce the initial position error in the background and has been shown to yield significant improvement in hurricane track forecasts in the earlier GFS version. However, Kleist et al., 2016 indicates that the relocation may lead to larger mean forecast track errors within longer forecast periods in the current GFS.

In this study, we investigate the impact of relocation in the GFS/GDAS system for the hurricane Joaquin (2015) case. As a first attempt, series of forecasts and DA experiments have been carried out with both regional and operational models. The capabilities of different DA schemes have been explored with the WRF model. To investigate the impact of relocation, a set of data assimilation experiments with and without the relocation have been carried out under an operational configuration with T670-T254 resolution. Results show that relocation not only corrects the forecast track but also influences the forecast hurricane structure and subsequent intensification. The mean GFS forecast without relocation has a deeper core structure and smaller track error after 72 hours of integration. This study reveals that although

the relocation scheme can reduce the initial position error in the background, it also can be harmful to the analysis and consequently affect the hurricane prediction.

## List of Figures

- Figure 2. 1** The single WRF model domain with 240×360 grids in horizontal, 36 levels in vertical, and the horizontal resolution of 21 km. ....19
- Figure 2. 2** WRF 5-day forecast track initialized from (a) 0000 UTC 29 Sep (blue), (b) 1200 UTC 29 Sep (red), (c) 0000 UTC 30 Sep (purple), (d) 1200 UTC 30 Sep (cyan), (e) 0000 UTC 01 Oct (green), and the NHC best track (black). ....20
- Figure 2. 3** WRF 5-day forecast track initialized at 1200 UTC 30 Sep for 36 ensembles (cyan). Ensemble mean track is presented as thick blue line and the thick black line represents the NHC best track.....22
- Figure 2. 4** Time series of intensity of WRF 5-day forecast initialized at 1200 UTC 30 Sep. (a) Central sea level pressure (top panel), and (b) Maximum wind speed (lower panel) of the best track (black), 36 ensemble forecasts (cyan), and the ensemble mean (blue). ....23
- Figure 2. 5** WRF 5-day forecast track initialized at 1200 UTC 30 Sep for configuration of (a) default (blue), (b) HWRF (red), (c) Manual (purple), and (d) NCAR Daily (cyan). ....24
- Figure 2. 6** A schematic of DA experiments. ....26
- Figure 2. 7** Analysis track initialized at 1200 UTC 30 September of (a) WRFDA 3DVAR (CV5) (blue), (b) WRFDA ETKF ens-mean (red), (c) WRFDA Hybrid (purple), (d) non-DA (cyan), (e) GSI 3DVAR (yellow), (f) GSI EnKF (green), and (g) NHC best track (black). ....28
- Figure 2. 8** Analysis hurricane intensity of (a) central sea level pressure (upper panel), and (b) maximum wind speed (lower panel) of WRFDA 3DVAR (CV5) (blue), WRFDA ETKF ens-mean (red), WRFDA Hybrid (purple), non-DA (cyan), GSI 3DVAR (yellow), GSI EnKF (green), and NHC best track (black). ....28
- Figure 2. 9** Vertical cross section of potential vorticity of analysis hurricane of experiments of (a) WRFDA hybrid, (b) No DA, (c) WRFDA 3DVAR with CV5, (d) WRFDA 3DVAR with CV3, and (d) GSI 3DVAR with NAM.....29
- Figure 3. 1** Best track (black) and the GFS 3-day forecast track initialized at 0000UTC Sep 28 (blue), 0000UTC Sep 29 (red), 0000UTC Sep 30 (purple), and 0000UTC Oct 01 (cyan) for (a) the Control, (b) the noRELOC, and (c) Operational.....34
- Figure 3. 2** The central sea level pressure of Joaquin of the Best track (black) and the GFS 3-day forecast for the Control (blue), the noRELOC (red), the Operational (purple), and the cnt\_GFS (green) which initialized at (a) 0000UTC Sep 30 and (b) 0000UTC Oct 01. ....35
- Figure 3. 3** The vertical cross section of the potential vorticity (color) and corresponding

potential temperature (dash line) for the GFS initial condition of (a) the Operational, and (c) the cnt\_GFS, and for the GFS 72-hr forecast of (b) the Operational and (d) the cnt\_GFS. ....35

**Figure 3. 4** (a) The Best track (black) and the GDAS analysis forecast track initialized at 0000UTC Sep 28 for the Control (blue) and the noRELOC (red). (b) The central sea level pressure of Joaquin of the Best track (black) and the GDAS analysis forecast for the Control (blue) and the noRELOC (red). .....37

**Figure 3. 5** The differences of relative vorticity (color) and MSLP (contour) between guess field and (a) 3-hr forecast, (b) 6-hr forecast, and (c) 9-hr forecast, between analysis and (d) 3-hr guess field, (e) 6-hr guess field, and (f) 9-hr guess field, and analysis between (h) 3-hr forecast, (i) 6-hr forecast, and (j) 9-hr forecast at 0000UTC Sep 30, 2015. ....38

**Figure 3. 6** The 850 mb wind speed (color) and MSLP (contour) for the (a) the guess field of Control and (b) the guess field of noRELOC, (d) the analysis field of Control and (e) the analysis field of noRELOC, the differences of (c) guess fields (Control - noRELOC), and (f) analysis fields (Control - noRELOC), (g) the analysis increment of Control and (h) the analysis increment of noRELOC , and (i) the difference of analysis increment (Control - noRELOC) at 0000UTC Sep 28, 2015. ....39

**Figure 3. 7** The 850 mb wind speed (color) and MSLP (contour) for the (a) the guess field of Control and (b) the guess field of noRELOC, (d) the analysis field of Control and (e) the analysis field of noRELOC, the differences of (c) guess fields (Control - noRELOC), and (f) analysis fields (Control - noRELOC), (g) the analysis increment of Control and (h) the analysis increment of noRELOC , and (i) the difference of analysis increment (Control - noRELOC) at 0000UTC Sep 30, 2015. ....40

**Figure 3. 8** The number of conventional observations used in the first DA loop at 0000UTC Sep 30 within (a) global domain, and (b) regional domain. ....42

**Figure 3. 9** The number of conventional observations used in the first DA loop at 0000UTC Oct 01 within (a) global domain, and (b) regional domain.....43

**Figure 3. 10** The O-B diagnosis differences (the Control – the noRELOC) within the regional domain of variable (a) PS (mb), (b) U (m/s), (c) Temperature (K), and (d) V (m/s) at 0000UTC Sep 30.....43

**Figure 3. 11** The GDAS analysis of wind field (wind barb), the mean SLP (contour), and the wind speed differences (the Control – the noRELOC) (color shaded) at 300 mb at 0000UTC Sep 30. Red and black color represent the Control and the noRELOC analysis, respectively. ....44

**Figure 3. 12** The GDAS analysis of wind field (wind barb), the mean SLP (contour), and the wind speed differences (the Control – the noRELOC) (colorshaded) at 1000 mb at 0000UTC Sep 30. Red and black color represent the Control and the noRELOC analysis, respectively. ....44

**Figure 3. 13** Number of radiance observations within the regional domain (shown in Figure

3.10) assimilated in the 1<sup>st</sup> iteration at 0000UTC Sep 30, 2015. The first and the second panels are the Control and the noRELOC EXP, respectively. The final panel is the number of observations difference (Control - noRELOC).....45

**Figure 3. 14** The brightness temperature (K) of the channel 4 of AMUSA (Metop-B) for (a) observation, (b) O-B (with bias correction) of the noRELOC, (c) O-B (with bias correction) of the Control, and (d) the O-B difference between the Control and noRELOC at 0000 UTC Sep 30, 2015. The black cross represents the observed hurricane center. ....46

**Figure 3. 15** The (a)(b)(c) horizontal differences of 850 mb specific humidity (color) and MSLP (contour), (e)(f)(g) 1-D cross section (yellow line) of the 850 mb specific humidity, and (h)(i)(j) vertical differences of 850 mb specific humidity (color) and wind speed (contour) at 0000UTC Sep 30, 2015. Left panel: Guess minus 6-hr forecast; middle panel: analysis minus Guess; right panel: analysis minus 6-hr forecast.....48

**Figure 3. 16** The MSLP (mb), 850 mb wind, and specific humidity (kg/kg) of (a) the forecast (6-hr), (b) the guess, (c) the analysis, (d) the difference between guess and the forecast, and (e) the vertical cross section of the yellow line in (d) at 0000UTC Sep 30, 2015. (f) is the analysis difference between the Control and the noRELOC. The blue cross and black cross in (a)(b)(c) represent the hurricane center of the Control forecast and the Best track, respectively. The green cross in (d) and (f) is the Best track hurricane center. The red and black triangles in (f) represent the analysis center of the Control and the noRELOC, respectively. ....49

**Figure 3. 17** The difference (Control - noRELOC) of the 850 mb temperature and the MSLP in (a) the forecast (6-hr), (b) the guess field, and (c) the analysis at 0000 UTC Sep 30, 2015.....49

**Figure 3. 18** The vertical cross section of the potential vorticity (color) and corresponding potential temperature (dash line) for the GFS (a) (c) 00-hr forecast and (b) (d) 72-hr forecast started from 0000 UTC Sep 30, 2015. The upper panel is the results of Control and the lower panel is the results of the noRELOC. ....50

**Figure 3. 19** The vertical cross section of the GDAS analysis of potential vorticity (color) and corresponding potential temperature (dash line) for (a) the Control, (b) the noRELOC, and (c) Operational at 0000UTC Oct 01.....51

**Figure 3. 20** The difference (Control - noRELOC) of 300 mb U wind of (a) the guess field, (b) the O-B (100-300 mb), and (c) the analysis at 0000 UTC Sep 28, 2015. The green cross is the Best tack hurricane center and the black cross is the forecast hurricane center.....52

**Figure 3. 21** Best track (black) and the GFS 5-day forecast track initialized at 0000UTC Sep 28 (blue), 0000UTC Sep 29 (red), 0000UTC Sep 30 (purple), and 0000UTC Oct 01 (cyan) for (a) the Control, and (b) the noRELOC.....53

**Figure 3. 22** The time series of (a) mean cross-track error, and (b) mean absolute-track error of the GFS 120-hr forecasts for the Control (blue) and the noRELOC (red) experiments

during Sep 29 to Oct 02, 2015. ....53

**Figure 3. 23** The vertical cross section of the potential vorticity (color) and corresponding potential temperature (dash line) for the GFS (a) (d) initial condition, (b) (e) 72-hr forecast, and (c)(e) 120-hr forecast, which initialized at 0000UTC Oct 01. The upper and lower panels represent the Control and the noRELOC, respectively. ....54

## List of Tables

<b>Table 2. 1</b>	Configuration tests of WRF forecast .....	23
<b>Table 2. 2</b>	Table of DA experiments .....	26
<b>Table 3. 1</b>	<b>Experimental Setups</b> .....	31
<b>Table 3. 2</b>	The configurations of operational data and DA experiments .....	32

## List of Abbreviations

DA	Data Assimilation
EnKF	Ensemble Kalman Filter
GDAS	Global Data Assimilation System
GFS	Global Forecast System
GFDL	Geophysical Fluid Dynamics Laboratory
GSI	Gridpoint Statistical Interpolation
NHC	National Hurricane Center
NWP	Numerical Weather Prediction
WRF	Weather Research and Forecasting model
WRFDA	Weather Research and Forecasting model Data Assimilation
SLP	Sea Level Pressure

# **1. Introduction**

## **1.1 Previous studies on hurricane initialization**

The official hurricane track forecast issued by National Hurricane Center (NHC) has shown significant improvement over the period 1970-98 with an annual rate of 1% -2% for 24-, 48-, and 72-h forecast periods (Franklin et al., 2003). The improvement primarily comes from the refinements of numerical models and initial conditions. The use of more available observation data (i.e. Satellite and aircraft) provides more information for the ocean regions and upper atmosphere, improving the initial conditions in the data assimilation, and therefore results in a more reliable model prediction. Despite the large improvement in data assimilation algorithms and more abundant observations, initializing the tropical cyclone properly as well as correcting the position errors in the background fields remains challenging. Historically, three general techniques that work together or alone have been developed for dealing with the hurricane initialization: data assimilation, dynamic initialization, and vortex bogusing.

Vortex bogusing has been proposed and extensively applied to the hurricane initialization for over two decades (Kurihara et al., 1993; Leslie and Holland, 1995; Pu and Braun, 2001; Kwon et al., 2002; Kwon and Cheong, 2010; Rappin et al., 2013). A typical vortex bogusing procedure includes three steps: (1) applying mathematical or statistical models to construct radial and vertical structures of the flow, (2) generating a synthetic

representation of the vortex, and (3) implanting or assimilating into the analysis. Compared to other methods, it is relatively simple, flexible, and cheap, which accounts for its popularity as a hurricane initialization option. However, there are several disadvantages of vortex bogusing. First, the synthetic vortex is usually not consistent with the model formulation; thus, additional spin-up time is necessary for the model to develop balanced flows (Pu and Braun, 2001). In addition, the symmetric characteristics of a synthetic vortex is not an appropriate assumption when the targeted hurricane has an asymmetric structure. Secondly, in order to insert the synthetic vortex, the existing vortex in the original model field must be removed. The vortex extraction is another challenging topic and may also induce model imbalance.

Another strategy for the hurricane initialization is data assimilation, which has been widely employed in the model initialization and shown significant improvement on the weather prediction. The main purpose of data assimilation is to optimally combine the background field and observations and obtain a more precise analysis field to improve the model initial condition. Generally, there are two major branches of DA, variational data assimilation and ensemble-based data assimilation. In recent years, the techniques of hybrid and EnVar, which combine the characteristics of variational and ensemble, are also widely used in the modern data assimilation systems. For variational system, the analysis is obtained by minimizing a cost function to approach the minimum of the analysis error. The analysis can be updated at a fixed time (i.e. 3D-Var) or within a short time interval by the use of an

adjoint model (i.e. 4D-Var). A disadvantage of 3D-Var is that the balance constraint (i.e. geostrophic balance) may be inappropriate for tropical cyclones, especially in the boundary layer, resulting in a physically unrealistic vortex (Hendricks et al., 2011). 4D-Var has been shown to be superior and has the capability to produce the primary and secondary circulations of tropical cyclones which are consistent with numerical model through the forward integration (Zou and Xiao, 2000). However, 4D-Var is computationally expensive and not easily portable.

Compared to the variational methods, initializing hurricanes using ensemble-based data assimilation is more straightforward. The technique of directly assimilating the tropical cyclone location into an EnKF has been proposed and proved to be promising for hurricane initialization (Chen and Snyder, 2006; Wu et al., 2010). In Chen and Snyder (2006), they proposed a simple linear updating scheme and showed that under the assumption of a small displacement of the forecast vortex, the non-Gaussian effects can be ignored and the observation operator can be treated as a procedure of searching the vortex center. Therefore, under appropriate assumptions, the information of the vortex center location can be assimilated with an EnKF and result in the correction of the position error in the background. Following this concept, Wu et al., (2010) successfully assimilated the tropical cyclone track (location) and structure data (10m wind from dropsounds) with the regional model (WRF) for real typhoon cases. Results show that the track and intensity forecasts have significantly

improved by directly assimilating the 10m wind structure (from dropsound) and the typhoon center locations.

Dealing with the position error problem is more complicated and challenging for variational data assimilation. For ensemble-based data assimilation, calculation of the observation operator can be substituted by covariances derived from ensemble statistics. For example, the  $\mathbf{P}^f \mathbf{H}^T = cov(\mathbf{x}^f, \mathbf{H}\mathbf{x}^f)$  and  $\mathbf{H}\mathbf{P}^f \mathbf{H}^T = cov(\mathbf{H}\mathbf{x}^f, \mathbf{H}\mathbf{x}^f)$  are approximated using sample covariances from the ensemble of model forecasts (Evensen 1994) instead of being computed directly. However, for variational data assimilation, the calculation of an observation operator for the tropical cyclone position and its adjoint is unavoidable. Therefore, how to properly prescribe these two components is a relatively difficult problem. Additionally, the tangent linear model which is associated with the cyclone position and used in variational analysis equations is also an obstacle. In general, the observation operator for cyclone position can be described as the process of searching the cyclone center. However, this searching process (i.e. searching for the minimum sea-level pressure) is usually non-differentiable and is not suitable for use in constructing the tangent linear model.

In recent years, many studies have proposed methods to solve the problem of reducing the position error with variational data assimilation. One of the notable approaches is the Feature Calibration and Alignment (FCA) technique (Nehrkorn et al., 2014). This method aims to correct the position error by adding small displacement vectors determined by feature

alignment on the background (control variables). As a result, the tropical cyclone can be gradually pushed to the target location by the add-on vectors through the inner loop iterations. In addition, they argued that the residual of the background errors would be smaller and more Gaussian by the use of the FCA. Other than computing additional displacement components discussed above, another approach proposed by Kepert (2009) is aimed to explore the possibility of directly assimilating the vortex location with variational data assimilation. In the Kepert (2009) study, the Holland analytic model (Holland, 1980) is applied to perform a 1-D tropical cyclone pressure profile as the background. This model is differentiable and used as the observation operator in the 3D-Var. By utilizing this model, the position information can be conveyed by the profile parameters and digested into the variational assimilation system. However, this study only applied the concept toward a simple 1-D profile model rather than to a forecast model integration; therefore, more studies are required to make this concept applicable.

For current operational NWP, the bogus vortex and tropical cyclone relocation scheme (Liu et al., 2000) are both utilized to correcting the initial position errors of tropical cyclones. In the operational GFS/GDAS system, the GFDL tracker (Marchok, 2002) program is running with the observed tropical cyclone vital data as a reference for identifying the tropical cyclone information in the GDAS forecast. If no tropical cyclone is found in the background forecast, then a bogus vortex will be generated (by assimilating a bogus wind

field). On the other hand, if the tropical cyclone is found but at an incorrect location, the relocation will be performed on the forecast field before assimilation is carried out. The relocation procedure first separates the forecast field into a basic field and a perturbation field (the latter consisting of hurricane and non-hurricane components) by applying the local filtering operator within a regional grid area. Next, the hurricane component is relocated (moved) to the advisory location and then superimposed on the environment field as well as the non-hurricane component to form a complete updated field (referred as guess field). The guess field with the relocated tropical cyclone will be applied to the subsequent assimilation process. More details about the relocation scheme in operational GFS can be found in Liu et al., 2000.

## **1.2 Motivation**

The relocation scheme has been used for operational NWP as a default procedure to deal with the hurricane initialization for many years. It has shown to significantly improve the hurricane prediction (Liu et al., 2000). However, Kleist et al., 2016 have found that the No-relocation runs generally yield better track forecasts beyond 24 hours. Statistically, the mean GFS forecast track error of the No-relocation case is nearly 35% smaller than the operational. The major object of this research is to investigate the impact of hurricane relocation on the GFS/GDAS system for the hurricane Joaquin (2015) case. Through this

study, we hope that we can provide useful information and contributions in operational hurricane prediction, further help to explore potential solutions for hurricane initialization, and eventually improve the general numerical weather prediction.

Beginning with the hurricane Joaquin (2015) case as a first attempt, we explored the capability of the regional model in handling the forecast of Joaquin with pure forecasts and different data assimilation schemes. In this part, different configurations in the WRF model and multiple data assimilation methods involved in WRFDA and GSI are applied and compared. The results of this part are discussed in the Chapter 2. As the main purpose of this study, we explored the impact of the relocation on the Joaquin case under an operational GDAS/GFS configuration (but with lower resolution). The influences of the relocation on the GDAS analysis and the GFS forecasts are investigated and discussed in Chapter 3. Finally, a brief summary and the future direction are given in Chapter 4.

## **2. The Impact of Different Data Assimilation Schemes on Hurricane Joaquin (2015) Case**

Before investigating the hurricane initialization with the operational system, we would like to gain a better understanding of the predictability, performance of different DA schemes, and sensitivity of different parameterization schemes for the Hurricane Joaquin (2015) case. In this chapter, the numerical regional model (Weather Research and Forecasting, WRF) and the DA systems, WRFDA and GSI, are applied to investigate the capability of handling the prediction of the hurricane Joaquin. A series of forecast runs has been carried out and various DA schemes have been tested. Details of the model configuration are described in section 2.1. Results of the WRF forecasts and performance of the DA schemes are discussed in section 2.2.

### **2.1 Model and Data**

In this chapter, the WRF v3.7.1 forecast model is utilized in combination with the WRFDA v3.7.1 and GSI v3.6 software to perform the DA cycling run. Experiments are run with a single domain of  $240 \times 360$  horizontal gridpoints and 36 sigma levels in the vertical. The horizontal model resolution is 21 km. A schematic of the model domain is shown as Figure 2.1. The initial and boundary conditions are generated from the NCEP FNL (Final) Operational Global Analysis data. Initial 36-member ensembles are perturbed by adding the

static 3DVAR error statistics (i.e. CV5 option) from WRFDA. The observed best track data are taken from National Hurricane Center (NHC) Best Track Data (HURDAT2) which provides six-hourly information on the hurricane location, maximum winds, central pressure, and the size of the tropical cyclones.

The DA systems, WRFDA v3.7.1 and GSI v3.6, are used to correct the model states with a six-hourly DA cycling. The applied DA schemes are listed in Table 2.2. For the DA experiments with the WRF model, we avoid assimilating satellite radiances due to the concern of radiance bias correction in the regional models and only assimilate the conventional observations from NCEP preBUFR data.

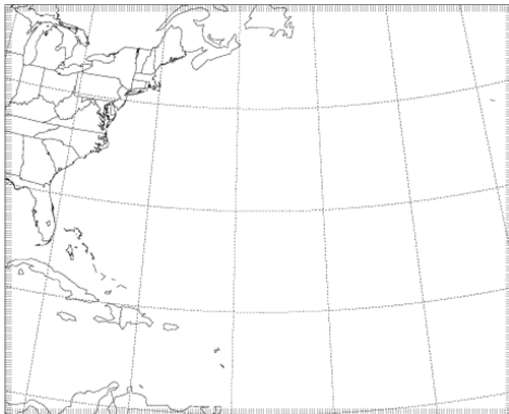


**Figure 2. 1** The single WRF model domain with 240×360 grids in horizontal, 36 levels in vertical, and the horizontal resolution of 21 km.

## 2.2 Deterministic and Ensemble 5-day forecasts of the Regional Model

A series of 5-day forecasts initialized at different times is carried out to explore the model capability of capturing the hairpin track of Joaquin. A track result with different initial

times is shown as Figure 2.2. It is apparent that the forecasts are not able to generate the hairpin track of Joaquin but instead they tend to move the storm toward the East coast. Our WRF track results are similar to much of the official model track forecasts (Berg (2016), Figure 9). In our case, it is difficult to predict the hairpin track of Joaquin, even for the late initialization at 0000 UTC 01 October.

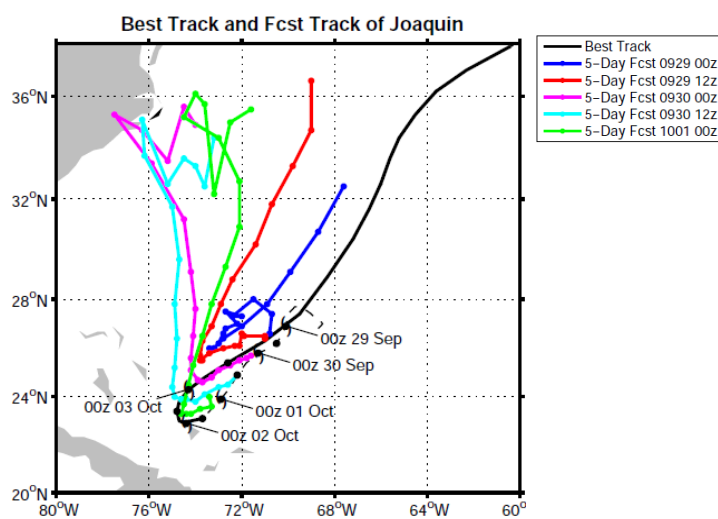


**Figure 2. 2** WRF 5-day forecast track initialized from (a) 0000 UTC 29 Sep (blue), (b) 1200 UTC 29 Sep (red), (c) 0000 UTC 30 Sep (purple), (d) 1200 UTC 30 Sep (cyan), (e) 0000 UTC 01 Oct (green), and the NHC best track (black).

Comparing the 500mb geopotential height field of the operational GFS analyses with the WRF 5-day forecast cold-started from GFS analysis at 0000UTC 30 September, we found that there are two significant differences that may lead to the incorrect northwestward direction in the track forecast. The first possible component is the trough and ridge location in the forecasts. The southward extension of ridge of the North Atlantic High in GFS analyses

prohibits the hurricane moving from northward and pushes it toward the south, while the same ridge in WRF-forecast locates relatively north. Without the involvement of data assimilation, the distribution of the trough and ridge system becomes significantly different after 3-days of forecast integration and it therefore affects the hurricane track direction.

The second possible reason for the incorrect track prediction is the hurricane intensity. The predicted hurricane is much weaker than the observed hurricane in all the forecast runs. As shown in Figure 2.4, the forecast hurricane became weaker and weaker, having difficulties sustaining its intensity at the tropical cyclone level, and it finally dissipated after 3 forecast days. During its weakening phase, it was attracted by the low system of the trough near the east coast of United States and tends to drift northwestward. Note that this northwestward drift also happened in the operational GFS forecast (Berg (2016)). In Berg (2016), he found that the GFS 120-hr forecast Joaquin is slightly further north than in the ECMWF 120-hr forecast, which makes it closer to the low pressure system associated with the trough near the east coast of United States, resulting in the northwestward movement of forecast Joaquin due to the attraction between two lows.

For the trial of ensemble forecast, the 36 initial ensembles are perturbed by adding perturbations generated from WRFDA (i.e. 3D-Var error statistics) to the GFS analysis and initialized at 1200 UTC 30 September. Results indicate that most of the ensembles failed to depict Joaquin's atypical southwestward motion toward the Bahamas from 0000 UTC 28

September through 1800 UTC 01 October (Figure 2.3).

In terms of the central sea-level pressure (SLP) and maximum 10m wind speed, Figure 2.4 shows that most of the ensemble members did not substantially strengthen; no members reached Category 3 hurricane intensity. Moreover, many of the ensemble vortices weakened as tropical storms (maximum wind speed < 104 km/h) after 0000 UTC 03 October. Hurricane Joaquin is a rapid intensification case which is hard to predict in current numerical models. There are several factors that would affect the prediction of rapid intensification, for example, the coupling effect of the air-sea interactions, the vertical environmental wind shear, and the low-level jet in inner core region. In addition, the mechanisms of rapid intensification are not completely known. Therefore, the inadequate capability of current forecast models in interpreting Joaquin's rapid intensification must be considered in this study.

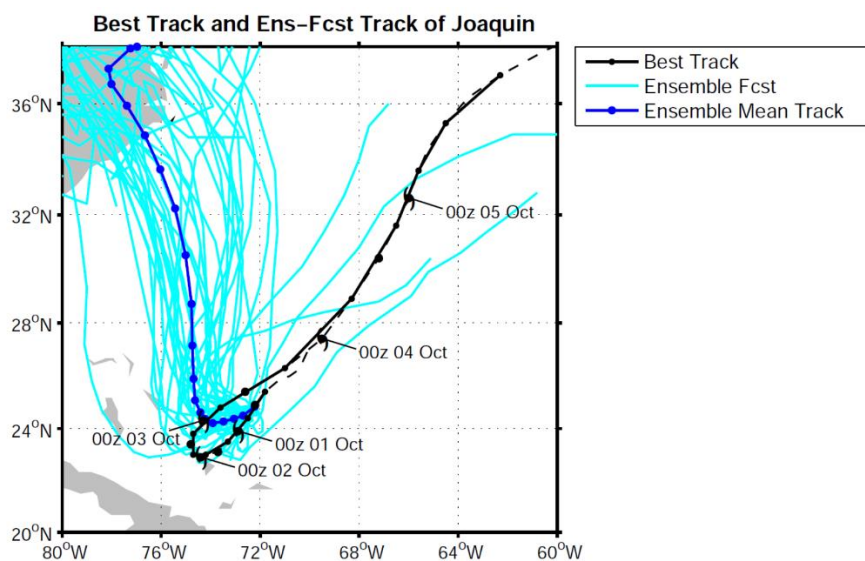


**Figure 2. 3** WRF 5-day forecast track initialized at 1200 UTC 30 Sep for 36 ensembles (cyan). Ensemble

mean track is presented as thick blue line and the thick black line represents the NHC best track.

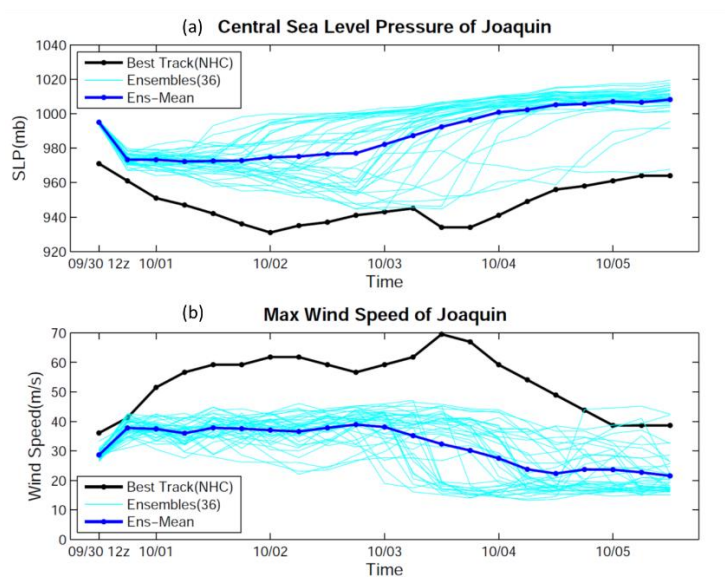


**Figure 2. 4** Time series of intensity of WRF 5-day forecast initialized at 1200 UTC 30 Sep. (a) Central sea level pressure (top panel), and (b) Maximum wind speed (lower panel) of the best track (black), 36 ensemble forecasts (cyan), and the ensemble mean (blue).

### 2.3 Impact of parameterization schemes on Joaquin prediction

We tested the WRF model forecasts with different parameterization configurations. Experiment settings are listed in **Table 2.1**. Results of the track are shown in Figure 2.5.

**Table 2. 1** Configuration tests of WRF forecast

EXP Name	Default	HWRP	NCAR Daily	Manual
<b>Description</b>	Currently used	NCAR's real-time hurricane runs in 2012	NCAR daily real-time runs over the US	Default but change the cu_physic
<b>Microphysics</b>	Lin et al. scheme	WRF Single-Moment 6-class scheme	New Thompson et al. scheme	Lin et al. scheme
<b>Longwave Radiation</b>	RRTM scheme	RRTMG scheme	RRTMG scheme	RRTM scheme
<b>Shortwave Radiation</b>	Dudhia scheme	RRTMG shortwave	RRTMG shortwave	Dudhia scheme
<b>Cumulus Parameterization</b>	Kain-Fritsch scheme	Tiedtke scheme (U. of Hawaii version)	Grell-Freitas (GF) scheme	New Simplified Arakawa-Schubert

Overall, all these configurations are not able to capture the hairpin track and rapid intensification of Joaquin, although different parameterization schemes have impacts on the prediction of the track and the intensity. Among these configurations, the HWRF configuration yields the best track result compared to other configurations. We would like to note that the performance of the parameterizations is influenced by many factors like model resolution. Since the resolution we utilize for our model is not very high, it would affect the performance of some of the parameterization schemes, especially for those associated with cloud physics. Therefore, more trials will be needed in the future to arrive at a more precise conclusion. Nevertheless, the results shown here can provide some insights into how the configurations can affect the track prediction and the importance of the parameterization in WRF model forecast on this Joaquin case.

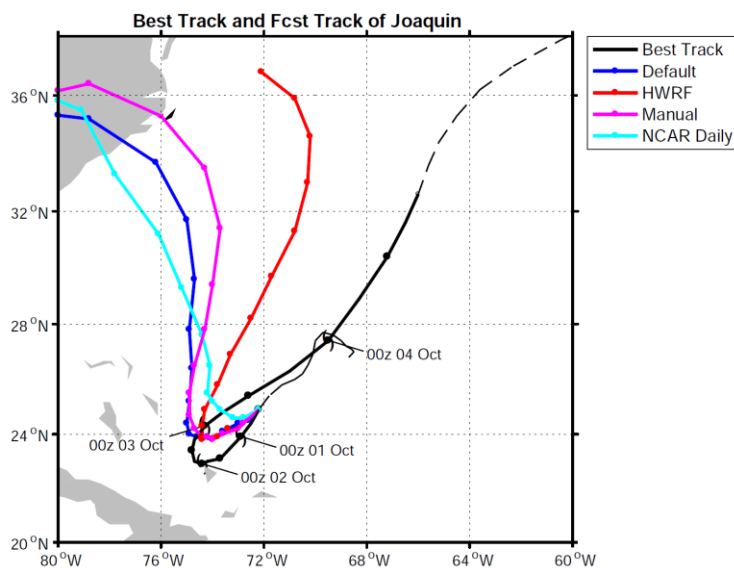


**Figure 2. 5** WRF 5-day forecast track initialized at 1200 UTC 30 Sep for configuration of (a) default (blue),

(b) HWRF (red), (c) Manual (purple), and (d) NCAR Daily (cyan).

## **2.4 The Impact of Regional Data Assimilation on Hurricane Joaquin (2015)**

The results in the previous sections highlight the importance and necessity of the involvement of the data assimilation in the hurricane prediction with the WRF model. In this section, we investigate the impact of different data assimilation schemes on the hurricane Joaquin case. For the DA experiments, WRF has been integrated with GSI and WRFDA as a joint DA system to perform DA cycling runs. Multiple DA schemes have been applied, such as 3D-Var, Ensemble Kalman Filter (EnKF), and Hybrid.

### **2.4.1 The Data Assimilation System and Experiment Setup**

In this section, two data assimilation systems have been applied, the WRFDA v3.7.1 and GSI v3.6. For the purpose of performing sequential DA cycling runs, the GSI-WRF DA system has been developed and tested. This system is designed for DA cycling run with WRF 6-hr forecast (single/ensembles) and GSI data assimilation (Var / EnKF). Details of the DA experiments can be found in Table 2.2.

The initial conditions (both single and ensembles) are generated from the GFS analysis at 0000UTC 30 September. The first data assimilation cycle begins at 0012UTC 30 September after a 12-hour model spin-up. The updating cycle is 6 hours and the DA experiments end at 0000UTC 05 October. For the EnKF ensembles initialization, details can be found in section

2.1. A schematic figure and details for the experiment setup can be found in Figure 2.6 and Table 2.2. Note that in both WRFDA and GSI, only conventional observations from NCEP preBUFR are assimilated.

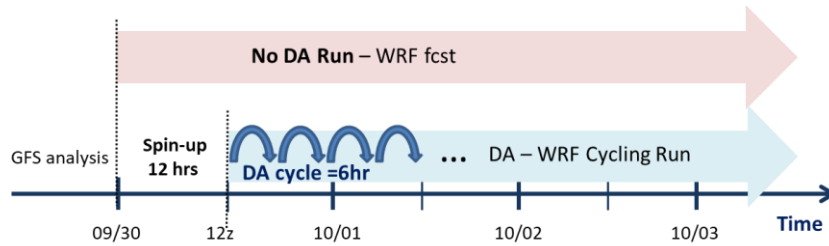


**Figure 2. 6** A schematic of DA experiments.

**Table 2. 2** Table of DA experiments

EXP name	DA System /Scheme		Description
<b>3DVAR</b>	WRFDA	3DVAR	With CV5 background error
<b>ETKF</b>		ETKF	36 ensembles, perturbed by adding errors generated from WRFDA (3DVAR error statistics)
<b>Hybrid</b>		Hybrid	50% 3DVAR + 50 % ETKF
<b>GSI 3DVAR</b>	GSI - WRF	3DVAR	With NAM background error statistic
<b>GSI EnKF</b>		EnKF	36 ensembles, perturbed by adding errors generated from WRFDA (3DVAR error statistics)
<b>No DA</b>	Pure WRF forecast		Cold start from FNL reanalysis

### 2.4.2 Real Case Experiments with WRF model: Joaquin (2015) case

A series of DA experiments have been carried out by utilizing GSI-WRF and WRFDA-WRF with schemes of 3D-Var, EnKF, and hybrid for investigating the impact of different DA schemes on the Joaquin case (Table 2.2).

We compare the result with the analysis hurricane track (Figure 2.7), intensity (Figure 2.8), and the structure (Figure 2.9). Overall, compared to the control run (No DA), the hurricane track is significantly improved by assimilating conventional observations. However, both the WRFDA and the GSI cycles bring Joaquin to the west of the Best Track positions and have difficulties in generating the rapid intensification over the 0000 UTC 30 September to 0000 UTC 02 October period, even though dropsonde data from the surrounding environment and inner core region have been assimilated (included as conventional sounding observations). As shown in Figure 2.8, all the analyzed hurricanes are too weak in contrast to the observed maximum wind and minimum SLP. Moreover, the analyzed TC structure (Figure 2.9) is also vertically shallow in much of the DA runs compared to the no-DA run. We also found that the analyzed structure of GSI with NAM background error covariance is weaker compared to the WRFDA outputs.

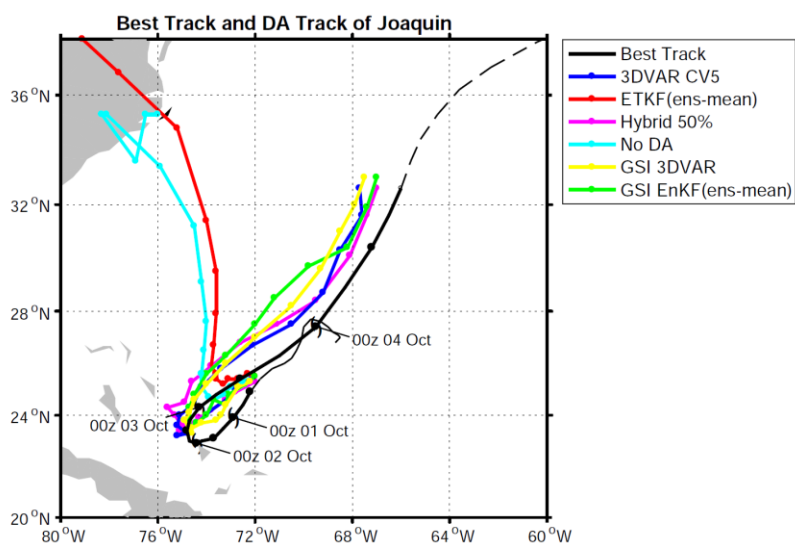


**Figure 2. 7** Analysis track initialized at 1200 UTC 30 September of (a) WRFDA 3DVAR (CV5) (blue), (b) WRFDA ETKF ens-mean (red), (c) WRFDA Hybrid (purple), (d) non-DA (cyan), (e) GSI 3DVAR (yellow), (f) GSI EnKF (green), and (g) NHC best track (black).

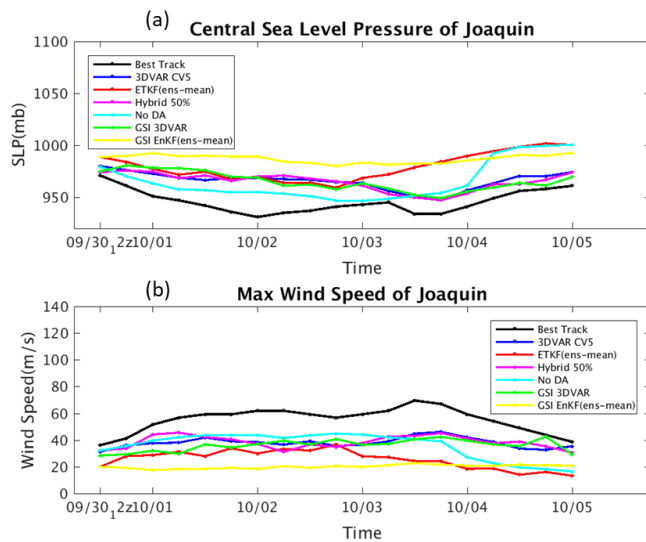


**Figure 2. 8** Analysis hurricane intensity of (a) central sea level pressure (upper panel), and (b) maximum wind speed (lower panel) of WRFDA 3DVAR (CV5) (blue), WRFDA ETKF ens-mean (red), WRFDA Hybrid (purple), non-DA (cyan), GSI 3DVAR (yellow), GSI EnKF (green), and NHC best track (black).

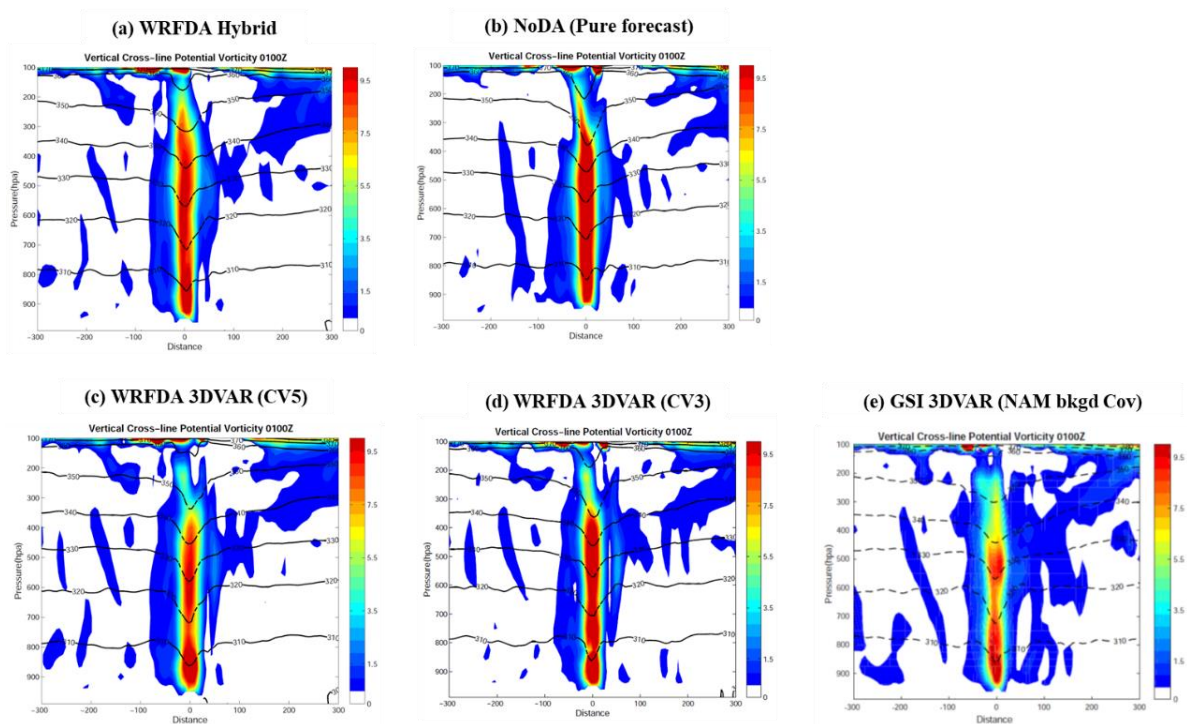


**Figure 2. 9** Vertical cross section of potential vorticity of analysis hurricane of experiments of (a) WRFDA hybrid, (b) No DA, (c) WRFDA 3DVAR with CV5, (d) WRFDA 3DVAR with CV3, and (e) GSI 3DVAR with NAM.

For the Joaquin case, the hurricane intensity would have a significant influence on the performance of its track. As discussed in Berg (2016), the deepening of the cyclone and the location of western Atlantic Ridge play important roles in predicting the southwestward motion of Joaquin. In ECMWF's forecast, Joaquin has a deeper structure compared to the GFS, with a deeper-layer flow subsequently pushing Joaquin southwestward (Berg, 2016). Therefore, in terms of dealing with the hurricane initialization problem, improving the deepening structure of Joaquin in its early generation will be one of the essential tasks in the prediction of Joaquin.

### **3. The Impact of the Relocation Scheme on the GFS/GDAS system**

In this part, the operational GDAS (Global Data Assimilation System)/ GFS (Global Forecast System) system with 4D-EnVar and 80 ensemble members (Wang et al. 2014; Kleist and Ide 2015) have been applied to investigate the impact of relocation scheme on the hurricane Joaquin (2015) case.

#### **3.1 Experimental Setup**

The model and data assimilation system applied in this study is the GFS / GDAS, a product from NCEP (National Centers for Environmental Prediction) EMC (Environmental Modeling Center). More information about GDAS/GFS can be found at <http://www.emc.ncep.noaa.gov/gmb/gdas/> and <http://www.emc.ncep.noaa.gov/GFS/>. The implementation we applied is a port of the NCEP 2016 operational version. The codes and scripts have been modified to work on a Linux machine and have been combined to work on NOAA S4. Tests showed that the small differences obtained from the port are within the noise level (reference: online user guide for the GDAS/GFS on S4, <https://groups.ssec.wisc.edu/groups/S4/s4-community-content/gdas-gfs-user-guide/?searchterm=GFS>).

In this study, two experiments have been carried out, the Control (with relocation) and the noRELOC (without relocation). The only difference between these two experiments is the use of the relocation scheme. A brief introduction of the relocation scheme can be found in

section 1.1. The configurations applied in this study follow the NCEP operational GFS/GDAS system (2016 version) on S4 but they are run with a lower resolution of T670-T254 due to the computational constraint. The experiment period runs from 0000 UTC Sep 21, which is one week in advance to the genesis of Hurricane Joaquin, to 0000 UTC Oct 05, 2015. Initial conditions are from operational GDAS analysis and they are downscaled to the resolution of T670. A chart of the relocation information is listed in Appendix I.

**Table 3.1 Experimental Setups**

<b>EXP name</b>	<b>Control</b>	<b>noRELOC</b>
<b>Relocation</b>	Yes	No
<b>DA System</b>	GDAS/GFS System on S4, with 4D-EnVar and 80 ensembles	
<b>Initial Condition</b>	Operational GDAS analysis (downscaled to T670)	
<b>Running Resolution</b>	T670 – T254	
<b>EXP Period</b>	0000 UTC Sep 21 to 0000 UTC Oct 05, 2015	

In the following discussion, we will examine the first relocation cycle (0000 UTC Sep 29, 2015) and mainly focus on the relocation cycle of 0000UTC Sep 30. The 0000 UTC Sep 30 cycle is significant because the largest relocation displacement (after reached tropical storm intensity) happened at this cycle and it is the beginning of the rapid intensification of Joaquin. Note that in the discussion below, the forecast field represents the 6-hr forecast integrated from the last DA cycle, the guess field is the output of the relocation and the input to the subsequent assimilation procedure (i.e. for the noRELOC, the forecast and the guess

field are the same).

### 3.2 Result comparison of Operational and the DA experiments

As a first step, we compared the analysis and forecast results obtained from the GDAS/GFS system on S4 with the Operational GDAS/GFS data (data downloaded from: <https://www.ncdc.noaa.gov/data-access/model-data/model-datasets/global-data-assimilation-system-gdas>) in order to gain a general understanding of the performance differences between our experiments and the operational forecast. Since one of the main configuration differences is the horizontal resolution, a series of GFS forecasts have been carried out to explore the impact of horizontal resolution for this case. The summary of the experimental settings is listed in Table 3.1.

**Table 3. 2** The configurations of operational data and DA experiments

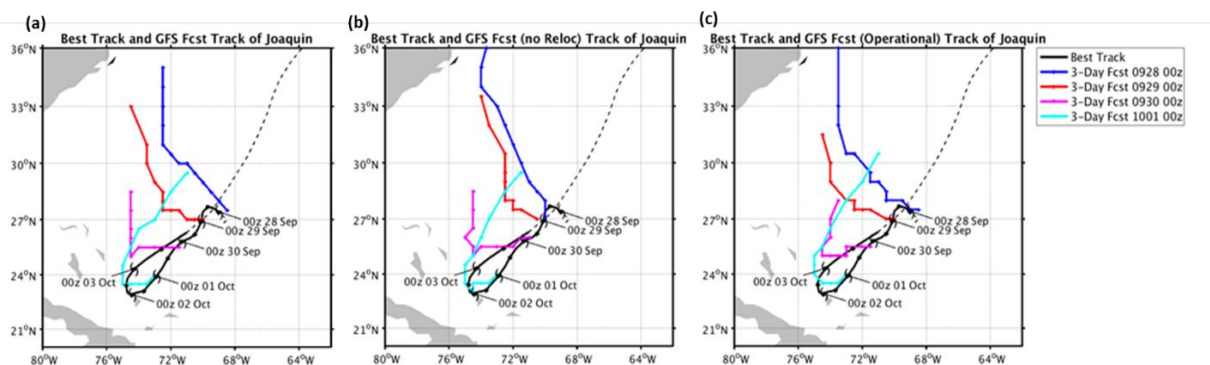
EXP name	Model description	Model running resolution	TC relocation	Output Resolution
cnt_Joaquin (Control)	GDAS/GFS on S4	T670 – T254	Yes	0.5 degree / 47 isobar level
noRELOC_Joaquin (noRELOC)		64 vertical levels	No	
Operational	Operational GDAS data	T1534 64 vertical levels	Yes	1.0 degree (for analysis) / 26 isobar level 0.25 degree (for GDAS 9-hr forecast)
cnt_GFS	GDAS/GFS on S4	T670 – T254 64 vertical levels	(Fcst only)	0.5 degree / 47 isobar level

Figure 3.1 (a), (b), and (c) shows the GFS forecast track initialized from 0000UTC Sep 28, Sep 29, Sep 30, and Oct 01 for the Control (a), noRELOC (b), and Operational (c), respectively. Results implied that the all the forecasts initialized before 0000 UTC Oct 01 failed to predict the southwestward hairpin track but instead generate a northwestward track moving toward the US east coast. Moreover, the forecast hurricanes initialized on 0000 UTC Sep 28 and 0000UTC Sep 29 are not able to develop and deepen enough to reach hurricane intensity (Figure 3.2).

The impact of the GFS running resolution can be assessed with the cnt\_GFS and Operational experiments, since the only difference between them is the running resolution (the output grid resolution is the same). The cnt\_GFS experiment is initialized with the operational GDAS analysis but the running resolution is reduced from T1534 to T670. Results of the comparison in the intensity and the structure between the Operational and cnt\_GFS can be found in Figure 3.2 and Figure 3.3. Figure 3.3 shows that even though both began with the same initial conditions, the 72-hr forecast hurricane structure of the cnt\_GFS struggles to 1) have the hurricane maximum 10m wind speed as strong as in the operational forecast and 2) have the hurricane central pressure deepen to 950 mb. This result indicates that the running resolution plays an important role in the hurricane development and that it would affect the performance of the hurricane intensification. With higher resolution, convective scale patterns associated with the tropical cyclone inner core dynamics can be

better interpreted and therefore provide a more realistic depiction of the tropical cyclone structure. Stronger convection in the inner core region provides more energy from a larger amount of latent heat release to further support tropical cyclone intensification. The importance of the running resolution in the hurricane forecast also has been mentioned in Zhang et al. 2016. In their study, they showed that the GFS track prediction of Hurricane Joaquin (2015) is significantly more accurate with higher vertical resolution.

Despite the fact that the running resolution applied in this study is lower than that of the operational GFS, we obtained very similar results for the forecast track (Figure 3.1) and the deepening trend (Figure 3.2) compared to the operational run. Therefore, we believe that the T670 resolution is sufficiently fine for exploring vortex relocation impacts on the Hurricane Joaquin (2015) case.



**Figure 3. 1** Best track (black) and the GFS 3-day forecast track initialized at 0000UTC Sep 28 (blue), 0000UTC Sep 29 (red), 0000UTC Sep 30 (purple), and 0000UTC Oct 01 (cyan) for (a) the Control, (b) the noRELOC, and (c) Operational.

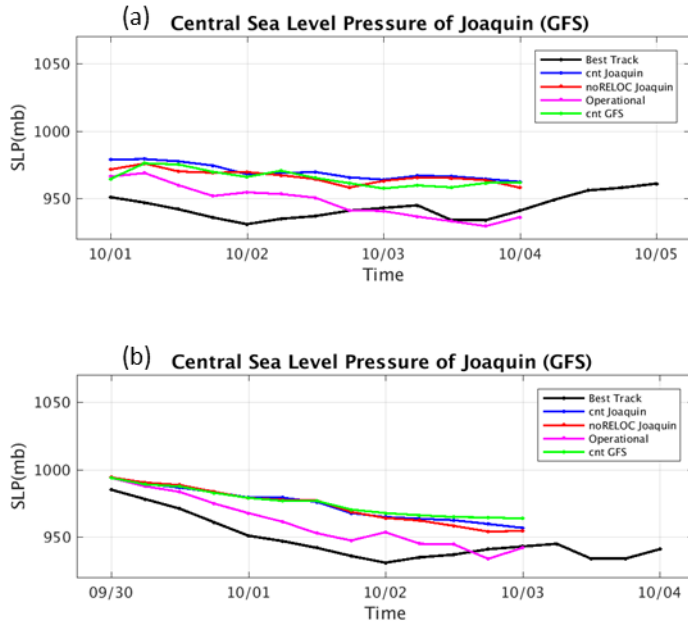


**Figure 3. 2** The central sea level pressure of Joaquin of the Best track (black) and the GFS 3-day forecast for the Control (blue), the noRELOC (red), the Operational (purple), and the cnt\_GFS (green) which initialized at (a) 0000UTC Sep 30 and (b) 0000UTC Oct 01.

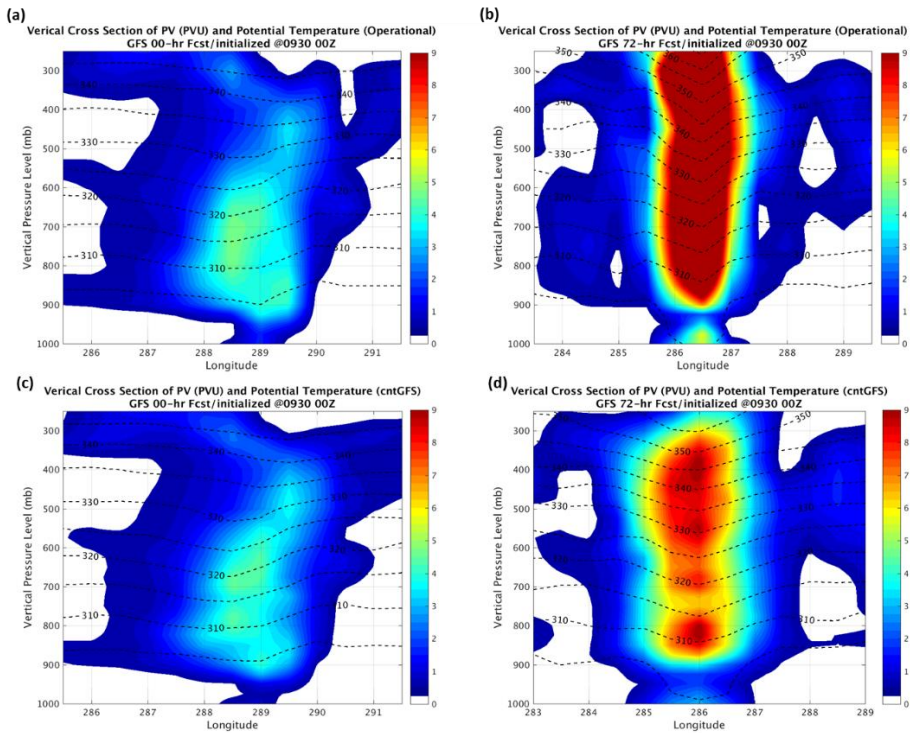


**Figure 3. 3** The vertical cross section of the potential vorticity (color) and corresponding potential temperature (dash line) for the GFS initial condition of (a) the Operational, and (c) the cnt\_GFS, and for the GFS 72-hr

forecast of (b) the Operational and (d) the cnt\_GFS.

### **3.2 Impact of relocation on GDAS analysis**

In this section, we compare the GDAS analyses generated by the Control and noRELOC experiments to investigate the impact of relocation on GDAS analysis. The experimental setup of Control and noRELOC is listed as Table 3.1.

The result of the analysis track is shown in Figure 3.4 (a). The analysis hurricane center locations are obtained from the GFDL Tracker v 3.9a and the Best Track position is from the NHC track data archive. Figure 3.4 (b) shows the central SLP analysis of the two experiments and the Best Track positions. In terms of the track analysis result, both the Control and the noRELOC perform reliable estimates of the hurricane location with a 6-hr DA cycling. Even though assimilating dropsonde and central SLP improves the analyzed hurricane structure and intensity, both DA experiments are still too weak compared to the Best track, in terms of central SLP, and both experiments have failed to simulate the rapid intensification of Joaquin between 1200UTC Sep 30<sup>th</sup> and 1200UTC Oct 01. As discussed in the section 3.2, the weak bias may be associated with the coarser running resolution that affects the rapid intensification of Joaquin. Note that for the 1800UTC Oct 03 DA cycle, no relocation took place due to an error in the operational TC vitals data conversion. To be consistent with the operational forecast, we ignore this error here and that is the reason why the hurricane

location at 1800UTC Oct 03 of the Control is not overlapped with the Best track in Figure 3.4

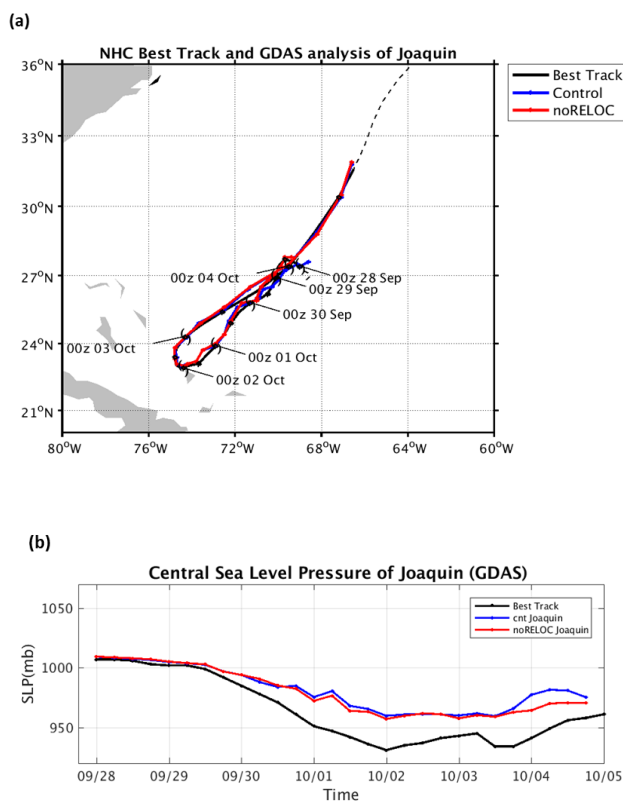


**Figure 3. 4** (a) The Best track (black) and the GDAS analysis forecast track initialized at 0000UTC Sep 28 for the Control (blue) and the noRELOC (red). (b) The central sea level pressure of Joaquin of the Best track (black) and the GDAS analysis forecast for the Control (blue) and the noRELOC (red).

Figures 3.5 shows the impact of the relocation on the analysis increments within one assimilation window. Due to the use of 4D-EnVar, the relocation information would exist in the time steps within the assimilation window like 3-hr and 9-hr increments and affect the analysis result. Comparisons of the analysis, the guess field, and the analysis increment between the Control and the noRELOC for the first relocation cycle (0000UTC Sep 28) and 0000 UTC Sep 30 are shown as Figure 3.6 and Figure 3.7, respectively. Although there is no

relocation in the noRELOC to correct the hurricane position, assimilating the central SLP also provides the information of the vortex center and consequently corrects the hurricane location through DA (Figure 3.6 (b)(e)(h)). Moreover, assimilating the hurricane central SLP in every DA cycle also helps to improve the hurricane intensity forecast (Figure 3.5 (h)).

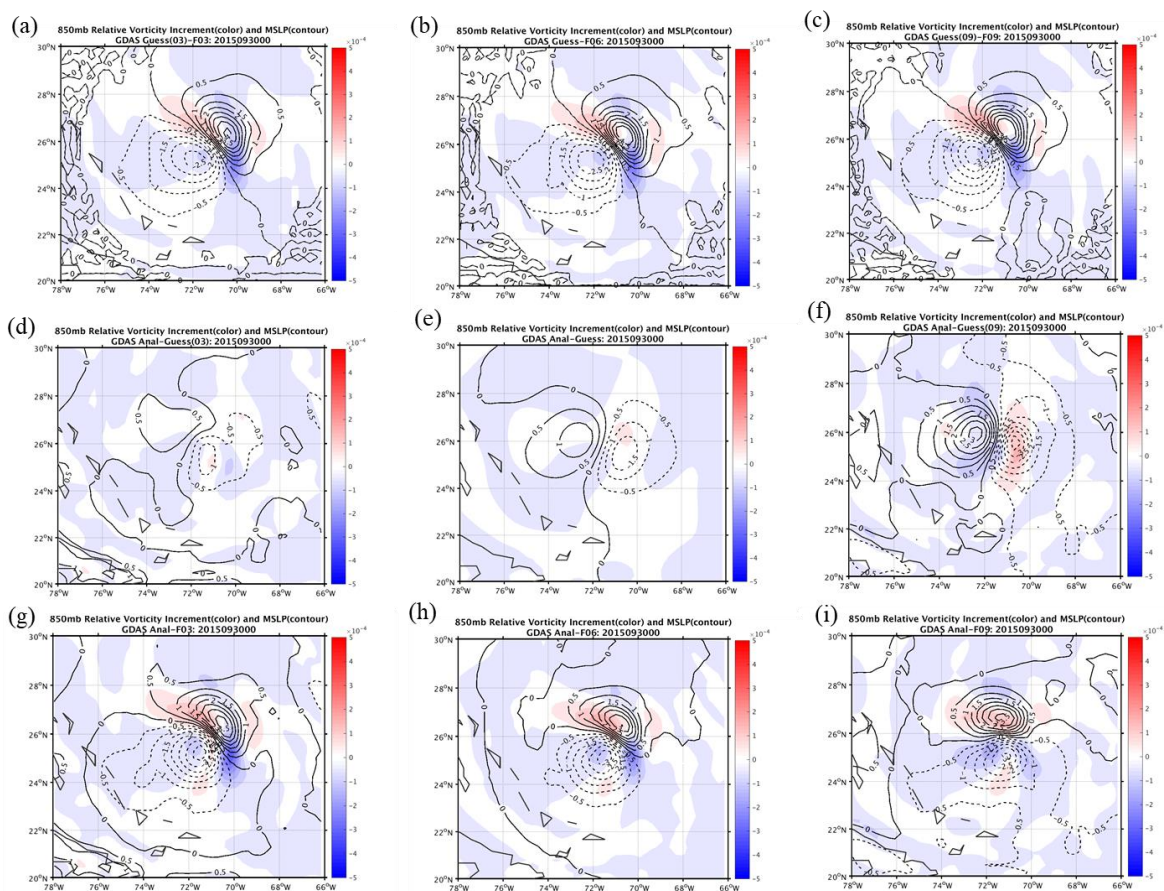


**Figure 3.5** The differences of relative vorticity (color) and MSLP (contour) between guess field and (a) 3-hr forecast, (b) 6-hr forecast, and (c) 9-hr forecast, between analysis and (d) 3-hr guess field, (e) 6-hr guess field, and (f) 9-hr guess field, and analysis between (h) 3-hr forecast, (i) 6-hr forecast, and (j) 9-hr forecast at 0000UTC Sep 30, 2015.

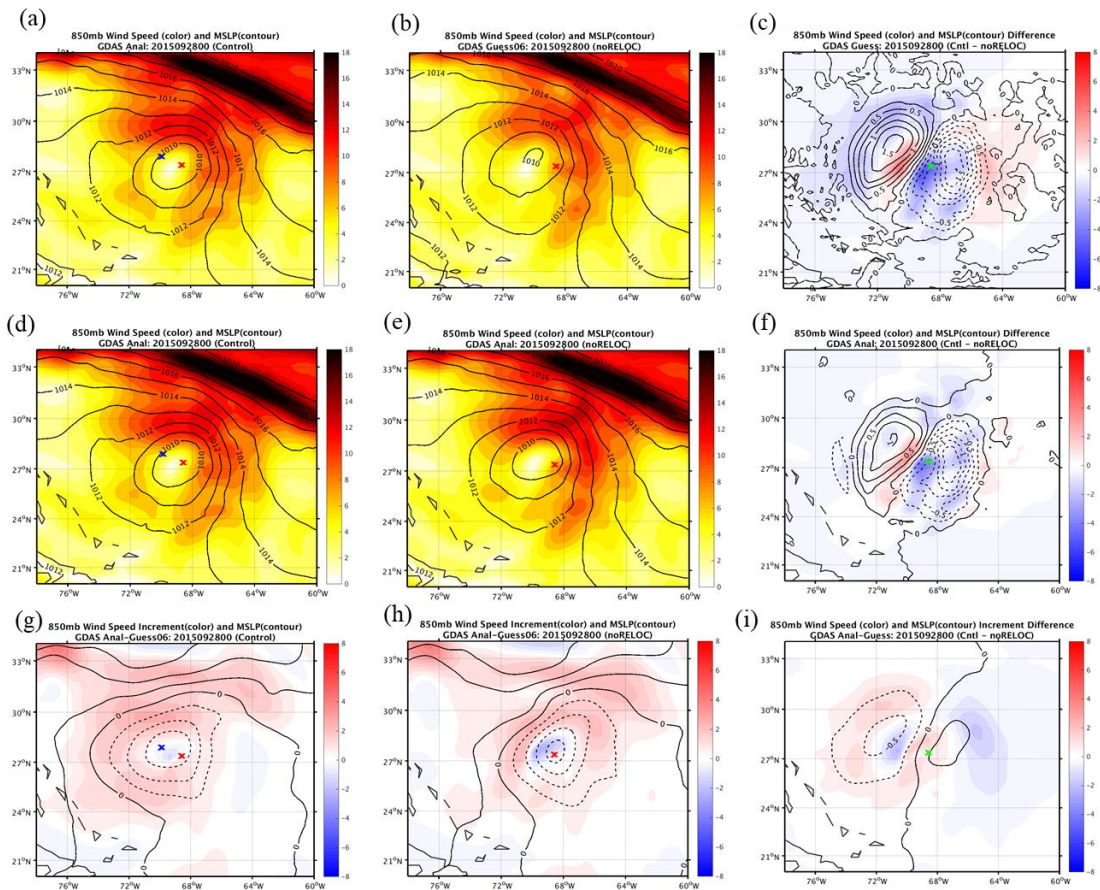


**Figure 3. 6** The 850 mb wind speed (color) and MSLP (contour) for the (a) the guess field of Control and (b) the guess field of noRELOC, (d) the analysis field of Control and (e) the analysis field of noRELOC, the differences of (c) guess fields (Control - noRELOC), and (f) analysis fields (Control - noRELOC), (g) the analysis increment of Control and (h) the analysis increment of noRELOC , and (i) the difference of analysis increment (Control - noRELOC) at 0000UTC Sep 28, 2015.

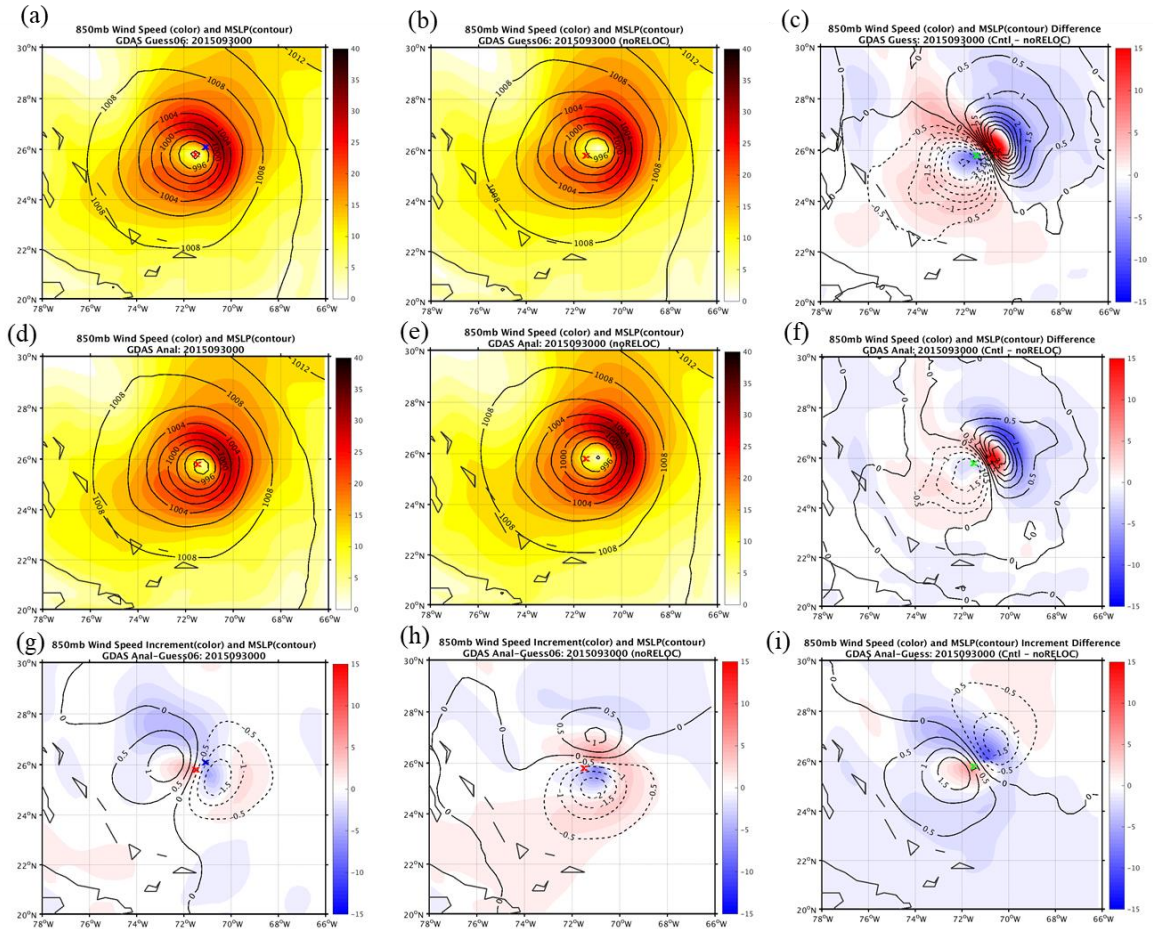


**Figure 3. 7** The 850 mb wind speed (color) and MSLP (contour) for the (a) the guess field of Control and (b) the guess field of noRELOC, (d) the analysis field of Control and (e) the analysis field of noRELOC, the differences of (c) guess fields (Control - noRELOC), and (f) analysis fields (Control - noRELOC), (g) the analysis increment of Control and (h) the analysis increment of noRELOC, and (i) the difference of analysis increment (Control - noRELOC) at 0000UTC Sep 30, 2015.

In the GDAS algorithm, relocation moves tropical cyclones to the corresponding observed locations and changes the guess field that is used in the subsequent observation quality control procedure. Therefore, the observation assimilated in the DA and the O-B statistics (i.e. the differences between the background and the observation at the observation

space) may be different due to the use of relocation. Figure 3.8 and Figure 3.9 compare the number of conventional observations used in the first outer loop at 0000UTC Sep 30 and 0000UTC Oct 01 for the Control (blue) and noRELOC (yellow) experiments. The regional area in panel (b) of Figure 3.8 and Figure 3.9 is defined by the region shown in Figure 3.10. The major differences in the number of observations used are for the variables U and V. Since the background circulation has been altered after relocation, the observation selection in the quality control procedure would also be different. Further, the O-B statistics would be different due to the different guess field that feeds into the DA system, resulting in statistical differences and that would influence the final analysis. The number of radiance observations assimilated for the Control and the noRELOC experiments is almost the same (Figure 3.13). However, changes in the temperature field due to relocation would affect the solution of the calculation of brightness temperature in the radiance transfer model, and consequently alter the O-B statistics. Figure 3.14 shows the observed brightness temperature of AMUSA on Metop-B (channel 4) and the O-B (with bias correction) statistics of the two DA experiments at 0000UTC Sep 30. The reason we pick channel 4 as an example is that it detects the temperature and humidity at the lowest layer of the troposphere (except for the surface). Figure 3.14 (d) shows a significant relocation pattern near the hurricane center in the O-B statistics differences.

A good example of how the O-B differences affect the analysis increment can be found

in Figure 3.10 and Figure 3.11, which show the O-B difference and analysis differences between the Control and noRELOC, respectively. There is a significant O-B difference near the Gulf of Mexico at the upper levels (Figure 3.10 (b) and (d)) which corresponds to the analysis wind speed differences that are associated with the jet stream flow at 300mb (Figure 3.11, at the left bottom). In this case, the relocation tends to shift the jet stream zone associated with the synoptic trough system and make it narrower and locally stronger. In addition to the upper level jet stream, the lower level stirring flow also changed, especially on the northwest and southwest side of the hurricane (Figure 3.12). As a result, the changes in the synoptic pattern will affect the environmental steering flow and therefore have impacts on the hurricane track forecast and development in the later stage.

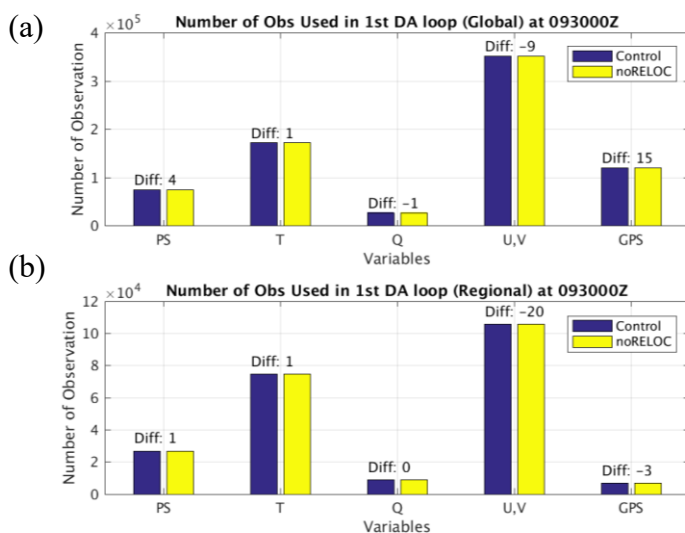


**Figure 3. 8** The number of conventional observations used in the first DA loop at 0000UTC Sep 30 within (a) global domain, and (b) regional domain.

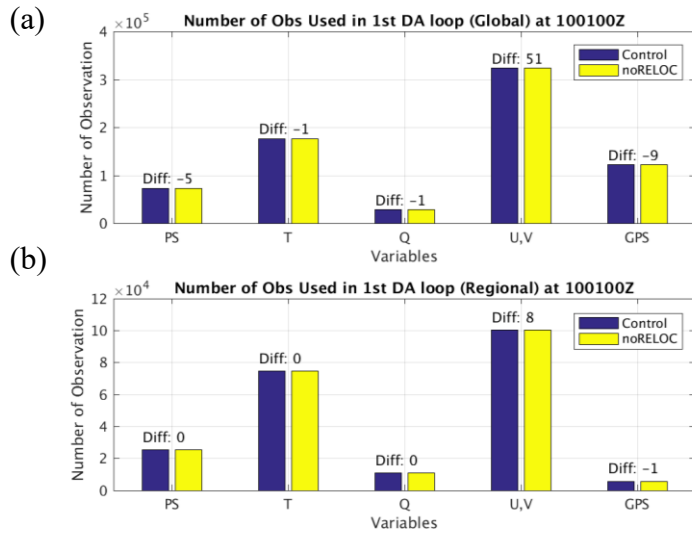


**Figure 3. 9** The number of conventional observations used in the first DA loop at 0000UTC Oct 01 within (a) global domain, and (b) regional domain.

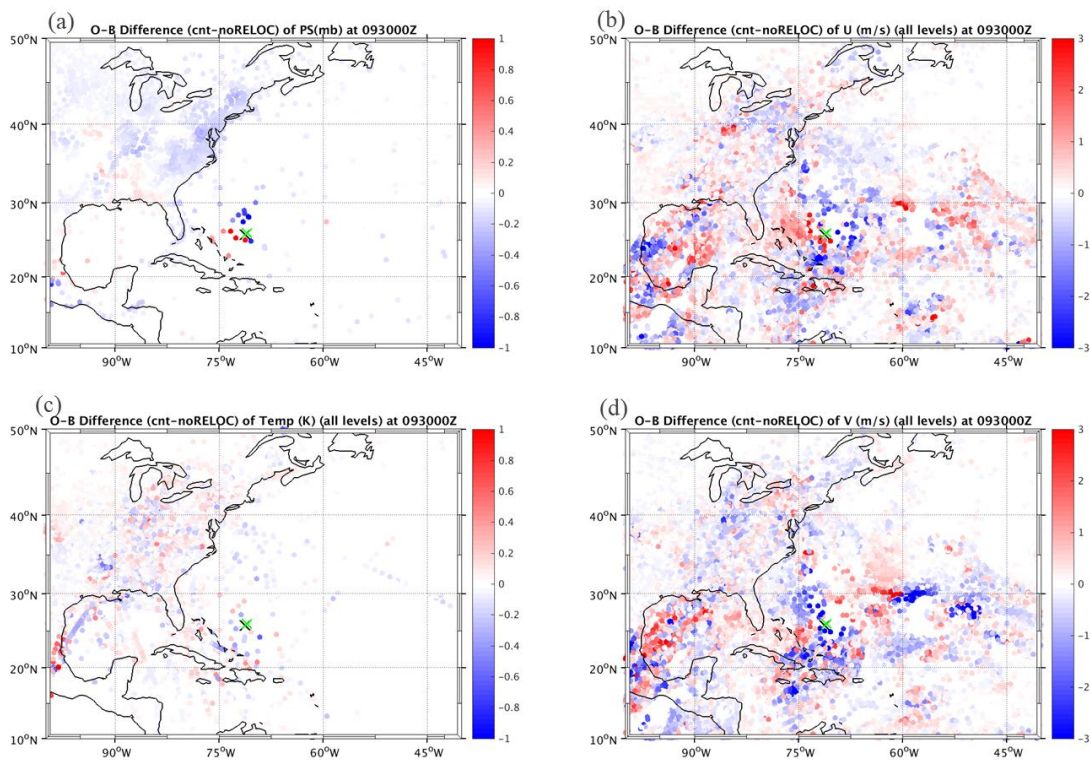


**Figure 3. 10** The O-B diagnosis differences (the Control – the noRELOC) within the regional domain of variable (a) PS (mb), (b) U (m/s), (c) Temperature (K), and (d) V (m/s) at 0000UTC Sep 30.

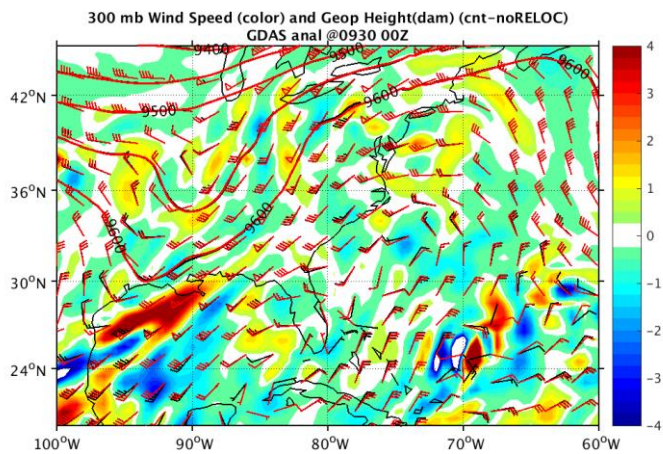


**Figure 3. 11** The GDAS analysis of wind field (wind barb), the mean SLP (contour), and the wind speed differences (the Control – the noRELOC) (color shaded) at 300 mb at 0000UTC Sep 30. Red and black color represent the Control and the noRELOC analysis, respectively.

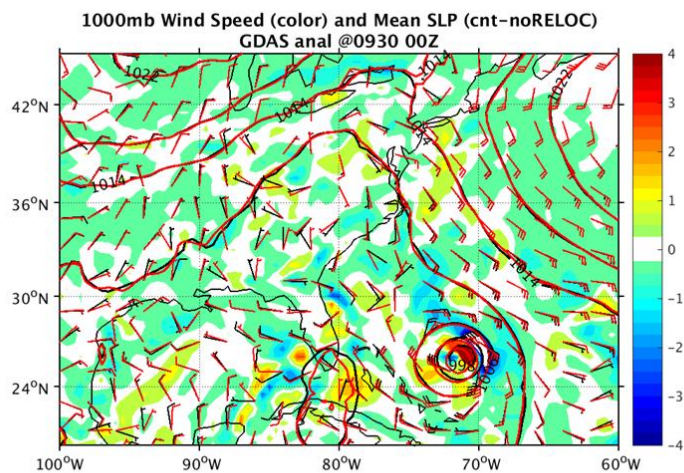


**Figure 3. 12** The GDAS analysis of wind field (wind barb), the mean SLP (contour), and the wind speed differences (the Control – the noRELOC) (colorshaded) at 1000 mb at 0000UTC Sep 30. Red and black color represent the Control and the noRELOC analysis, respectively.

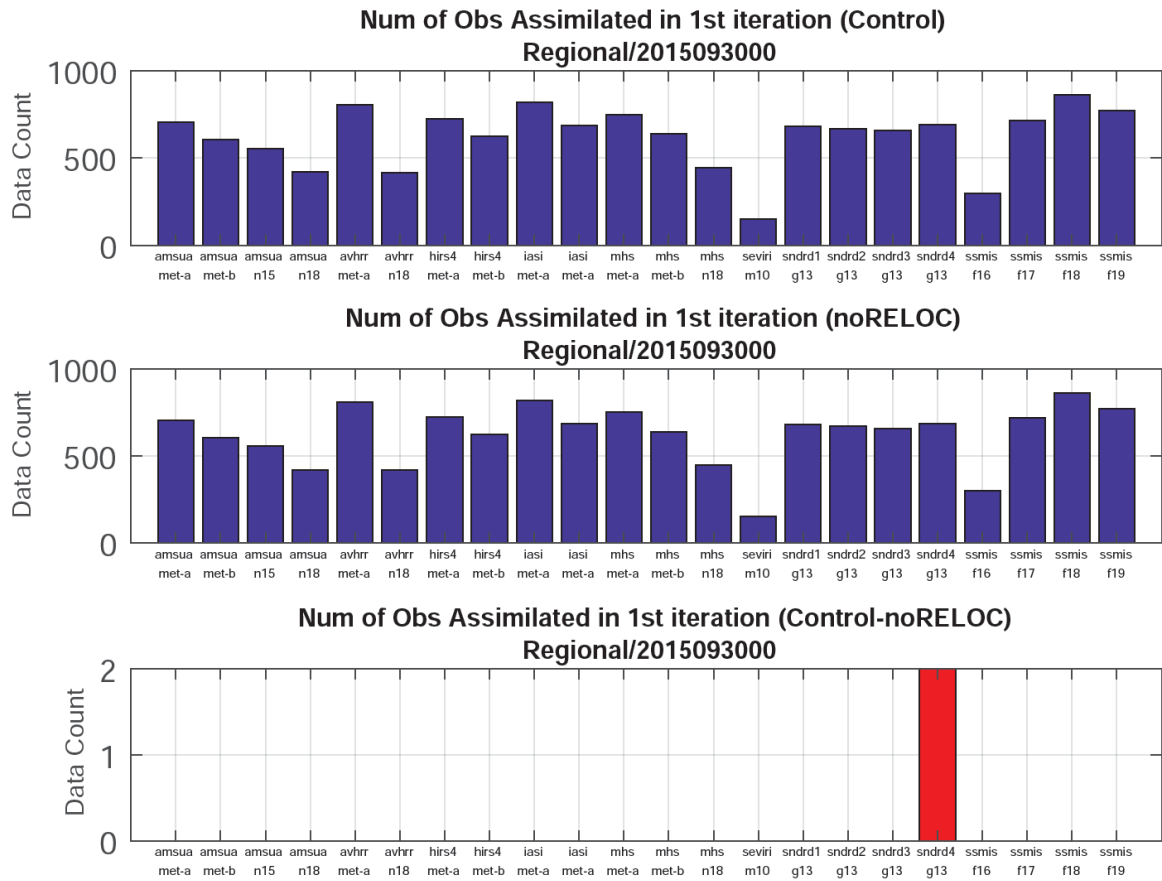


**Figure 3.13** Number of radiance observations within the regional domain (shown in Figure 3.10) assimilated in the 1<sup>st</sup> iteration at 0000UTC Sep 30, 2015. The first and the second panels are the Control and the noRELOC EXP, respectively. The final panel is the number of observations difference (Control - noRELOC).

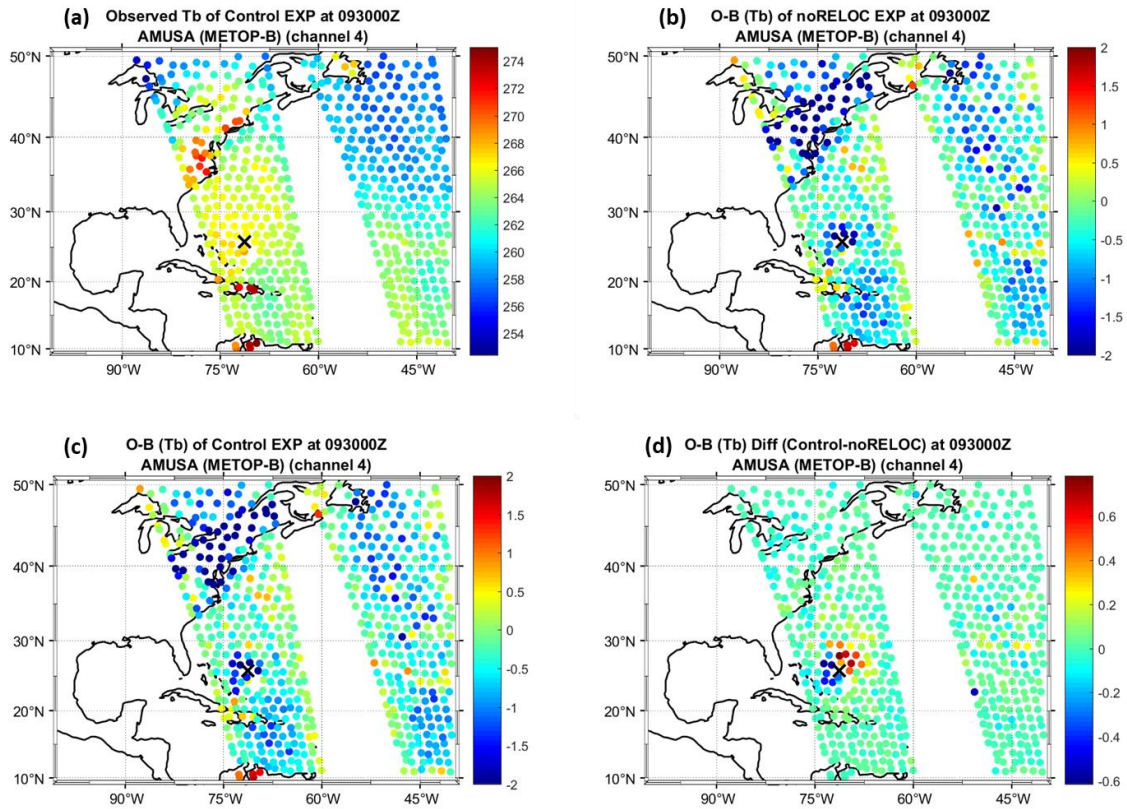


**Figure 3. 14** The brightness temperature (K) of the channel 4 of AMUSA (Metop-B) for (a) observation, (b) O-B (with bias correction) of the noRELOC, (c) O-B (with bias correction) of the Control, and (d) the O-B difference between the Control and noRELOC at 0000 UTC Sep 30, 2015. The black cross represents the observed hurricane center.

The changes in the analysis humidity environment is another good example of how relocation can affect the analysis increment as well as the analyzed hurricane structure (Figure 3.15 and Figure 3.16). The humidity, which is related to the latent heat source and is associated with the hurricane intensification, is an important component to investigate, especially for the analysis cycle of 0000UTC Sep 30 since it is the day that Joaquin reached hurricane intensity and began its rapid intensification. Figure 3.15 shows the horizontal and

vertical impacts of relocation on the humidity increment at 0000UTC Sep 30. It is apparent that the environment near the hurricane became drier after relocation (Figure 3.15 (a)). Even though data assimilation tended to provide a positive impact on the humidity correction (Figure 3.15 (h)), the dry impacts from the relocation remain in the final analysis increment (Figure 3.15 (i)). Comparing the analysis result with the noRELOC, the 850mb specific humidity field of the Control analysis is significantly drier near the hurricane center (Figure 3.16 (f)). Moreover, the Control analysis also has significant drier impact at multiple analysis cycles that have larger relocation displacements, such as 0000UTC Sep 28, and 1200UTC Sep 30 (Figure not shown). As mentioned in the previous studies related to the rapid intensification hurricane cases (Smith et al. 2017; Montgomery and Smith 2012), the requirement of sufficient moisture in the inner core region is one of the important components of thermodynamic support for hurricane spin-up. The dry analysis increment would cause a drier environment in the inner core region and inhibit the rapid intensification of the hurricane. In addition to the humidity, the 850mb temperature field also has a cooling impact after the relocation at the DA cycle of 0000 UTC Sep 30. Figure 3.17 shows Control and noRELOC differences (Control - noRELOC) in 850 mb temperature in the forecast, the guess field, and the analysis. It is apparent that the difference in the temperature becomes more significant after the relocation (Figure 3.17 (a)(b)), which indicates a cooler background near the core region in the Control. This cooler environment in the Control remains after the

analysis and it could possibly affect the hurricane intensification in the GFS forecast initialized from 0000 UTC Sep 30 as shown in Figure 3.18.

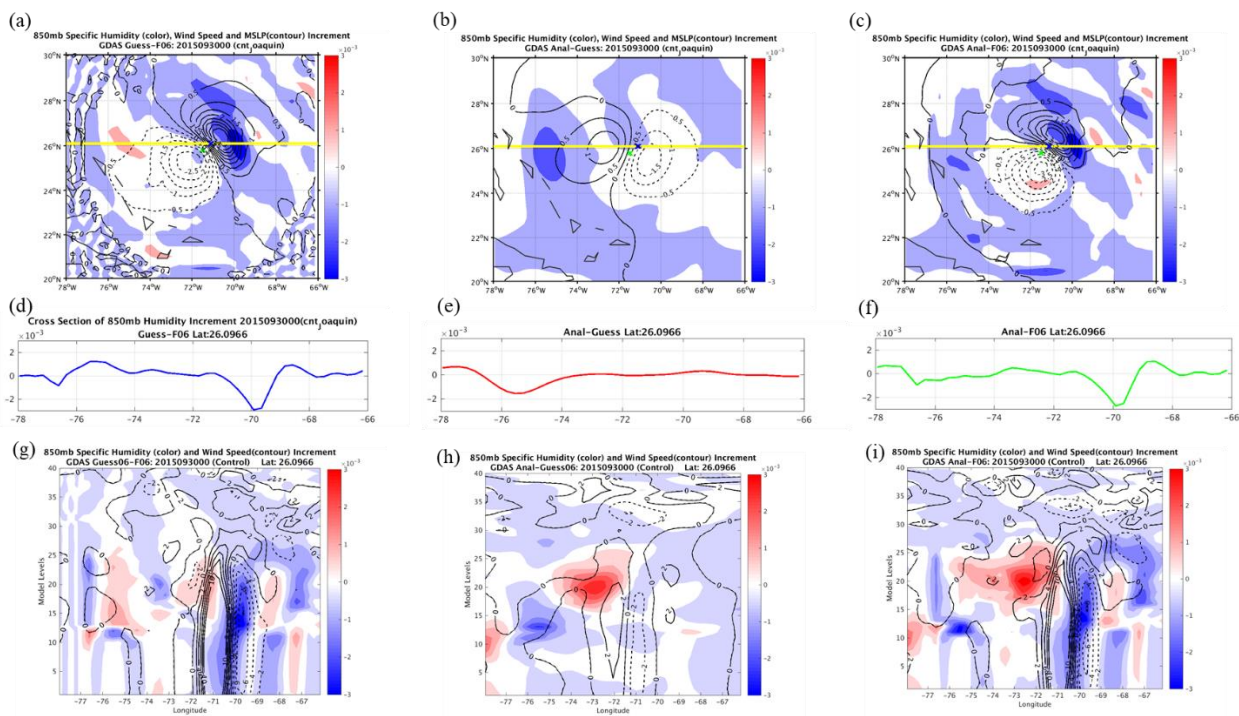


**Figure 3. 15** The (a)(b)(c) horizontal differences of 850 mb specific humidity (color) and MSLP (contour), (e)(f)(g) 1-D cross section (yellow line) of the 850 mb specific humidity, and (h)(i)(j) vertical differences of 850 mb specific humidity (color) and wind speed (contour) at 0000UTC Sep 30, 2015. Left panel: Guess minus 6-hr forecast; middle panel: analysis minus Guess; right panel: analysis minus 6-hr forecast.

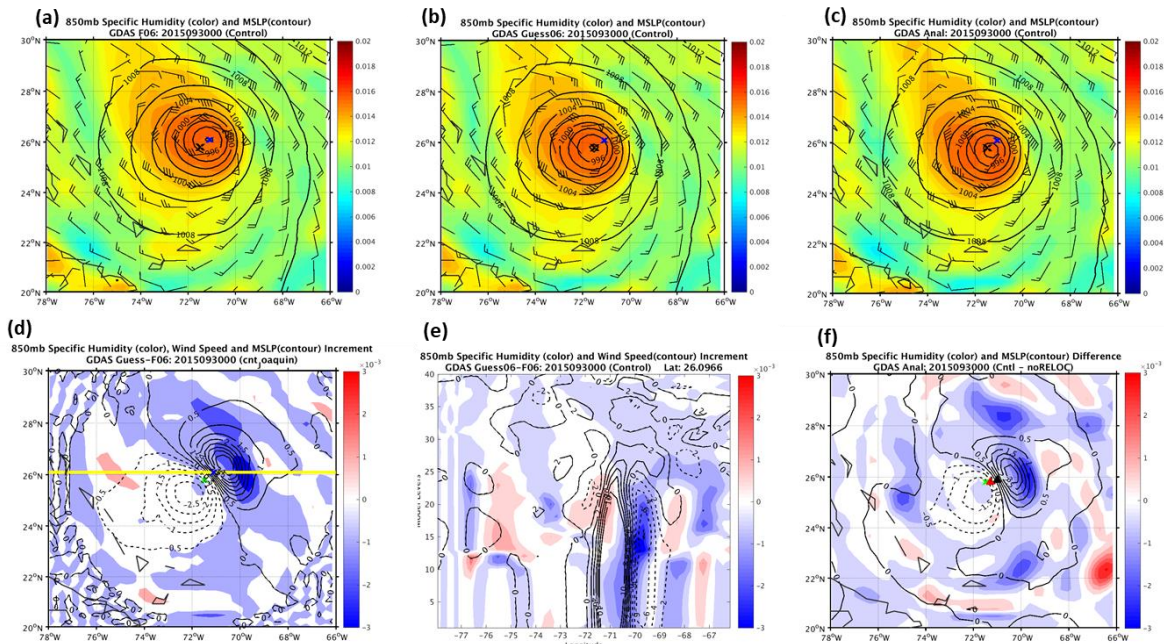


**Figure 3. 16** The MSLP (mb), 850 mb wind, and specific humidity (kg/kg) of (a) the forecast (6-hr), (b) the guess, (c) the analysis, (d) the difference between guess and the forecast, and (e) the vertical cross section of the yellow line in (d) at 0000UTC Sep 30, 2015. (f) is the analysis difference between the Control and the noRELOC. The blue cross and black cross in (a)(b)(c) represent the hurricane center of the Control forecast and the Best track, respectively. The green cross in (d) and (f) is the Best track hurricane center. The red and black triangles in (f) represent the analysis center of the Control and the noRELOC, respectively.

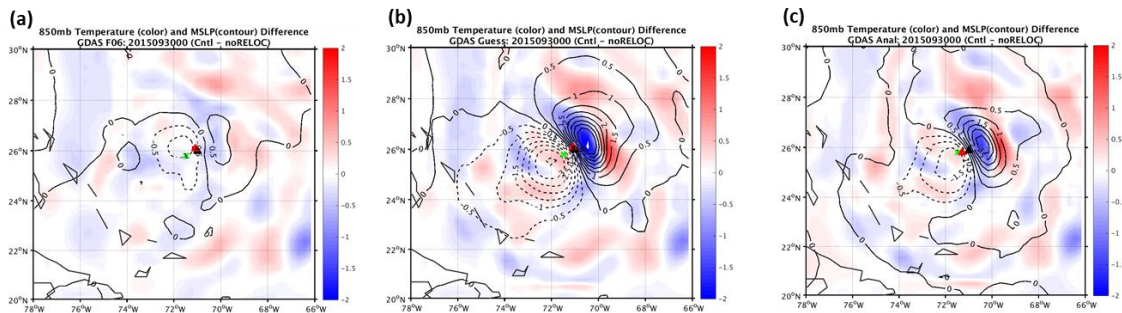


**Figure 3. 17** The difference (Control - noRELOC) of the 850 mb temperature and the MSLP in (a) the forecast (6-hr), (b) the guess field, and (c) the analysis at 0000 UTC Sep 30, 2015.

A comparison of the analyzed hurricane vertical PV structure in the Control, the noRELOC, and the operational experiments at 0000UTC Oct 01 is shown as Figure 3.19. The

result implies that the noRELOC has significantly better development and deeper structure than the Control, especially in the layer of  $\sim 800$ mb. With a more accurate hurricane structure, noRELOC can be expected to generate a more reliable GFS forecast (results shown in section 3.3). However, the analyses of both experiments are not deepening Joaquin enough compared to the operational forecast, in which the coarser running is one of the possible reasons.

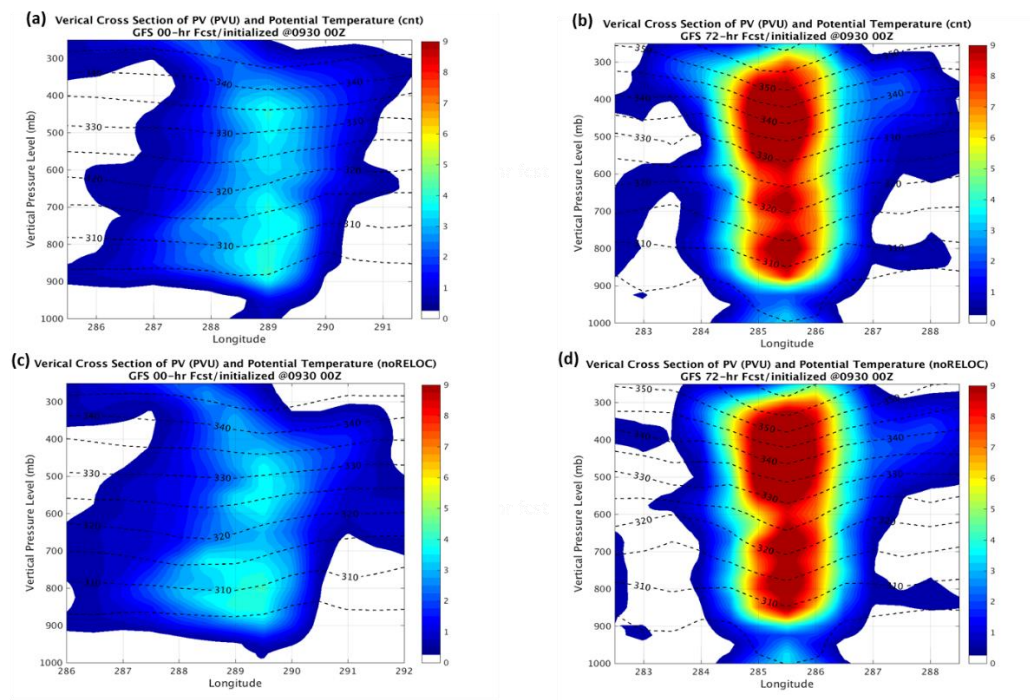


**Figure 3. 18** The vertical cross section of the potential vorticity (color) and corresponding potential temperature (dash line) for the GFS (a) (c) 00-hr forecast and (b) (d) 72-hr forecast started from 0000 UTC Sep 30, 2015. The upper panel is the results of Control and the lower panel is the results of the noRELOC.

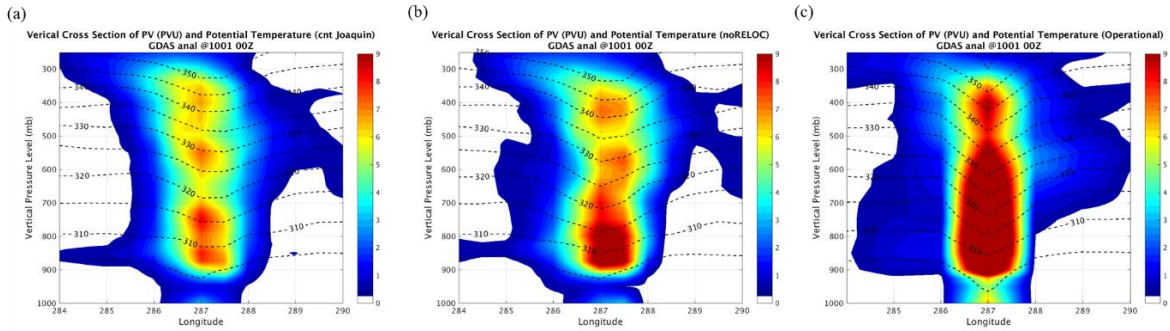


**Figure 3. 19** The vertical cross section of the GDAS analysis of potential vorticity (color) and corresponding potential temperature (dash line) for (a) the Control, (b) the noRELOC, and (c) Operational at 0000UTC Oct 01.

In addition, we found that the relocation would affect the upper level even when the cyclone is in fact shallow and weak. Figure 3.20 shows the difference (Control - noRELOC) of the 300 mb U field at the first relocation cycle (0000 UTC Sep 28, 2015). For the first relocation cycle, the forecasts (i.e. field before relocation) of the noRELOC and the Control are the same such that the difference in the guess fields (i.e. field after relocation) come from the relocation. At 0000 UTC Sep 28, Joaquin had just attained tropical depression status. At this early stage, the cyclone structure was still shallow and weak and had not extended to the upper levels (i.e. 300 mb). However, relocation perturbed the upper level vortex structure as shown in Figure 3.20 (a). The perturbation due to the relocation would affect the O-B (Figure 3.20 (b)) and remain in the analysis (Figure 3.20 (c)).

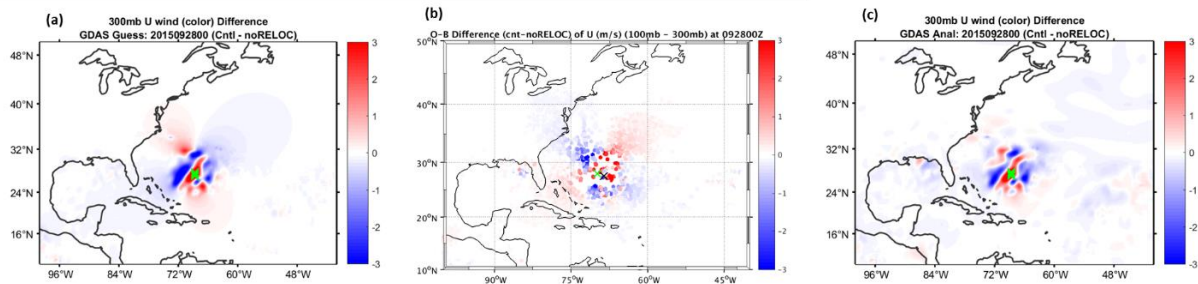


**Figure 3. 20** The difference (Control - noRELOC) of 300 mb U wind of (a) the guess field, (b) the O-B (100-300 mb), and (c) the analysis at 0000 UTC Sep 28, 2015. The green cross is the Best tack hurricane center and the black cross is the forecast hurricane center.

### 3.3 Impact of the relocation on the GFS forecast

Although previous studies have claimed that relocation can correct the position error in the background and improve the hurricane analysis and prediction (Liu et al., 2000), it also can have harmful impacts on the analysis and consequently lead to a worse track forecast with a longer lead time (Kleist et al., 2016). In the Joaquin (2015) case, we also found the same situation as indicated in Kleist et al. 2016. Figure 3.21 shows the 5-day Control and noRELOC GFS track forecasts initialized from 0000UTC Sep 29, 0000UTC Sep 30, 0000UTC Oct 01, and 0000UTC Oct 02, respectively. Figure 3.22 shows the mean track error of the four forecasts shown in Figure 3.21 for the two experiments. The mean absolute- and cross- track errors of noRELOC GFS forecast are significantly smaller than those of Control, especially after the 72-hour lead time. As we discussed in the previous section, although the relocation corrected the position error in the background, altering the guess field would also affect the O-B statistics in the assimilation and it could be harmful to the environment and

hurricane structure analysis.

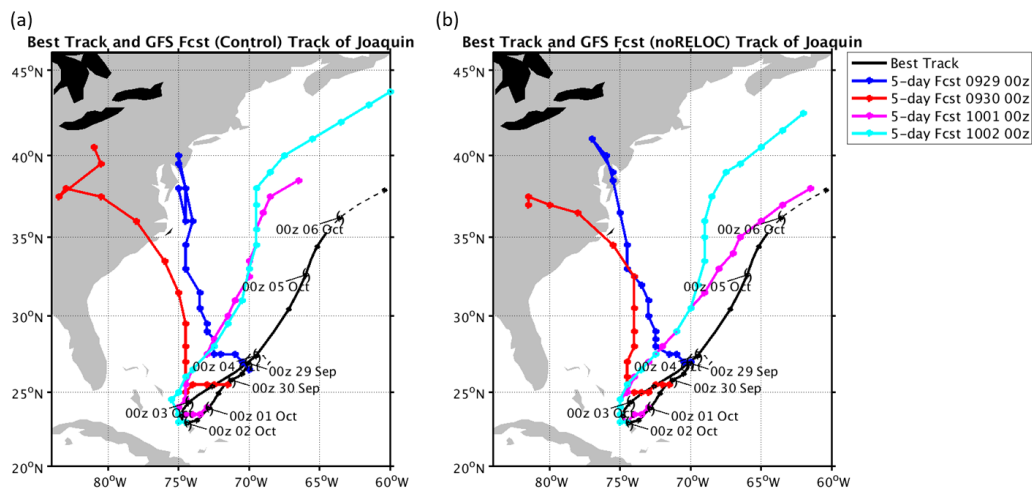


**Figure 3. 21** Best track (black) and the GFS 5-day forecast track initialized at 0000UTC Sep 28 (blue), 0000UTC Sep 29 (red), 0000UTC Sep 30 (purple), and 0000UTC Oct 01 (cyan) for (a) the Control, and (b) the noRELOC.

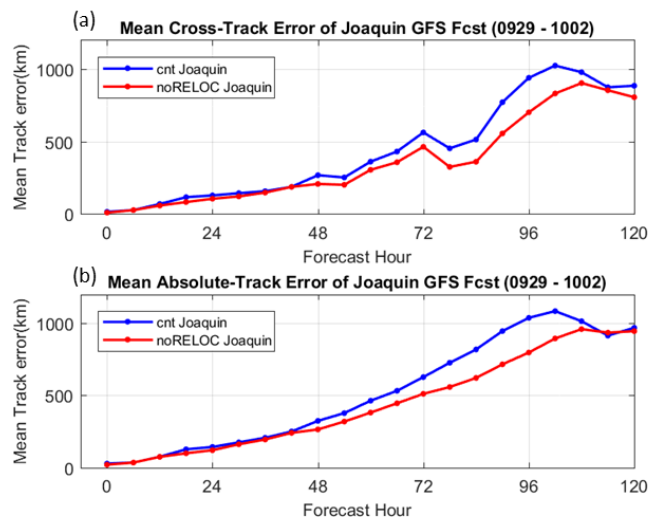


**Figure 3. 22** The time series of (a) mean cross-track error, and (b) mean absolute-track error of the GFS 120-hr forecasts for the Control (blue) and the noRELOC (red) experiments during Sep 29 to Oct 02, 2015.

The hurricane structure in the GFS 00-hr, 72-hr, and 120-hr forecasts initialized from 0000 UTC Oct 01 for the two experiments is shown in Figure 3.23. With a more reliable estimate of the hurricane structure as an initial condition, the hurricane structure of the noRELOC indicates a better development compared to Control after a 72-hr forecast. Note that the 120-hr forecast hurricane in both experiments has transitioned into an extratropical cyclone; thus the warm core structure at the lower levels has weakened and disappeared (Figure 3.23 (c) and (f)).

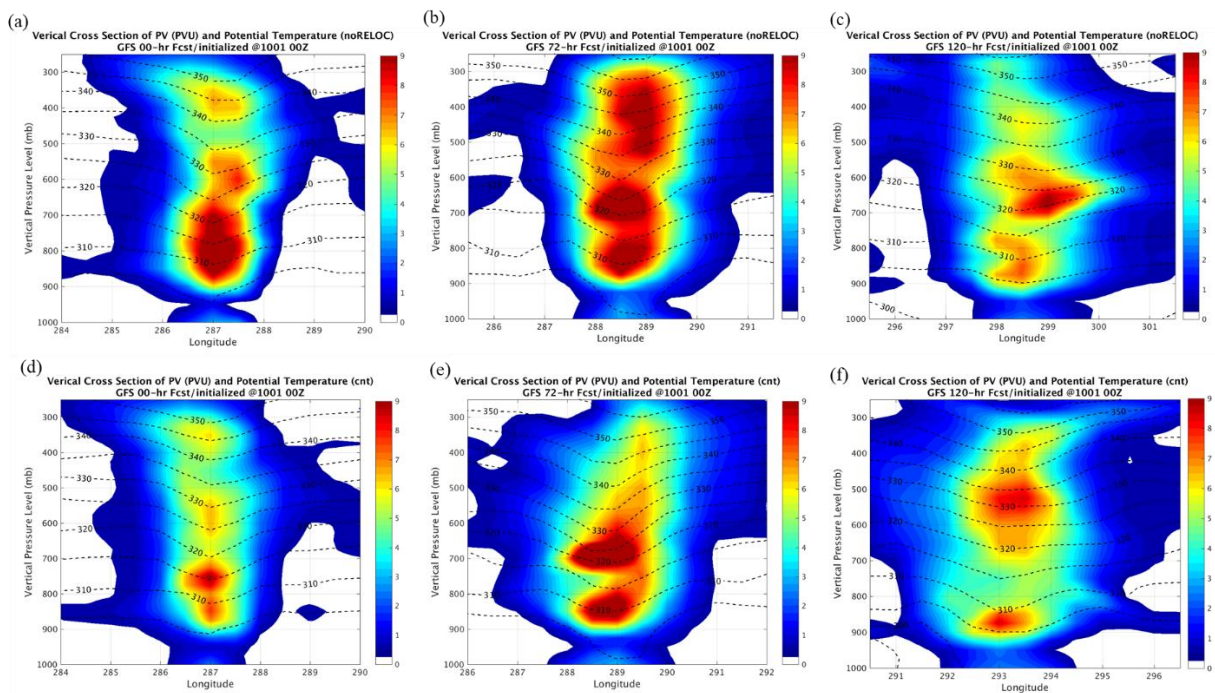


**Figure 3. 23** The vertical cross section of the potential vorticity (color) and corresponding potential temperature (dash line) for the GFS (a) (d) initial condition, (b) (e) 72-hr forecast, and (c)(e) 120-hr forecast, which initialized at 0000UTC Oct 01. The upper and lower panels represent the Control and the noRELOC, respectively.

## 4. Conclusion

### 4.1 Summary of Research

In this study, a series of DA experiments have been carried out to investigate the performance of regional and operational DA systems in the problem of hurricane prediction and initialization. As a first attempt, the regional WRF model has been utilized in the forecast and the DA experiments. We found that the track forecasts of hurricane Joaquin are sensitive to different parameterization schemes in WRF. Among all the configuration options, the HWRF configuration has the best performance in the track prediction. However, even with the HWRF configuration, we still failed to capture the atypical hairpin track of Joaquin at the early stage. Furthermore, the poor performance of the hurricane intensity in WRF forecasts also indicates that the hurricane is not able to successfully develop in the model integration, even with the analysis cold start. Therefore, the involvement of data assimilation is essentially necessary to improve the model state.

In order to explore the performance of different DA schemes in handling the Joaquin case, we compare the analysis results of 3D-Var, ETKF, and Hybrid in WRFDA and 3D-Var and EnKF in GSI. Track results show that most of these schemes are able to correct the track and generate a hairpin track. However, all of the analysis tracks have a westward displacement compared to the Best Track. In terms of the intensity, all DA schemes failed to depict the first rapid intensification period (Sep 30 to Oct 02) of Joaquin but they

demonstrated the subsequent second intensification period (Oct 03 to Oct 04). Note that the overall analysis hurricanes are still weaker than the observed minimum SLP.

For the second part of this study, we explore the impact of the relocation scheme on GDAS/GFS analysis and forecasts. Although relocation is capable of reducing the initial position error in the background, it could be harmful to the analysis. We found that the relocation has an influence on the lower level steering flow and the upper level jet. In the Joaquin case, the upper level jet stream became narrower and locally stronger after relocation. These changes in the jet stream are expected to have impacts on the development of the low system associated with the trough near the east coast of US and as a result affect the synoptic pattern after few days. Taking the changes in the jet stream as an example, we found that this change is consistent with the O-B statistics differences in the wind field. Since the relocation altered the background state, the O-B calculation would also be different. As a result, the analysis state changes, even for areas that are not close to the hurricane. Another issue of relocation that we found in the Joaquin case is the humidity and temperature increment. We found that the inner core region in the background became significantly drier and cooler after the relocation at some analysis cycles. These dry and cold signals would remain in the analysis and consequently affect the forecast hurricane development, especially for the rapid intensification that partially depends on the inner core dynamics. With less moisture, and therefore less latent heat release, the efficiency of the hurricane development would be

influenced and lead to a weaker structure. Although the overall environment is not continuously drier over the hurricane lifetime period, the dry pattern in the core region due to the relocation happened at the beginning of the rapid intensification period on Sep 30 and therefore would prohibit the hurricane from undergoing rapid intensification.

Relocation not only affects the GDAS analysis but also impacts the GFS track forecasts with long lead time. In the Joaquin case, we discovered that the track error of the relocation case is larger than the non-relocation case after a 72-hr forecast. Additionally, the forecast hurricane without relocation is stronger than that with the relocation after 72-hr integration. This result of the GFS forecast again indicates that the relocation could be harmful to the analysis and therefore could consequently lead to a worse forecast.

## **4.2 Future Direction**

While the Hurricane Joaquin case is a good example of how relocation can affect the hurricane analysis and forecast, more different types of hurricane cases should be included in the future experiments to obtain a more comprehensive understanding and robust conclusion.

Another issue in dealing with the hurricane initialization is the running resolution. The running resolution plays an important role in hurricane development due to the performance of the cloud physics and the inner core dynamics. For a hurricane rapid intensification case like Joaquin, a finer resolution is necessary for providing a better representation of the non-balanced dynamics in the inner core region within the boundary layer. In addition, the

impact of the relocation would be expected to differ with running resolution. We have not explored the effect of different resolution on the relocation and the hurricane initialization due to the computational resource limitations, but we recommend considering the impact of resolution on the hurricane initialization problem.

Based on the current result we analyzed, we would suggest reconsidering the necessity of using relocation in the operational GDAS DA system. Instead of utilizing the relocation, other methods such as the Feature Calibration and Alignment (FCA) technique (Nehrkorn et al., 2014) in WRFDA or the technique of assimilating the TC center in an EnKF are potential solutions to reduce the initial position error. However, how to appropriately apply these concepts on the operational 4D-EnVar system would be another challenging topic that needs to be explored.

### **4.3 Acknowledgements**

The support of NOAA NWS grant (NGGPS/R2O) NA15NWS4680017 is gratefully acknowledged. The support of S4 at the University of Wisconsin-Madison for high-performance computing is greatly appreciated.

## Reference

- Chen, Y., & Snyder, C. (2007). Assimilating vortex position with an ensemble Kalman filter. *Monthly Weather Review*, 135(5), 1828-1845.
- Evensen, G. (1994). Sequential data assimilation with a nonlinear quasi-geostrophic model using Monte Carlo methods to forecast error statistics. *Journal of Geophysical Research: Oceans*, 99(C5), 10143-10162.
- Franklin, J. L., McAdie, C. J., & Lawrence, M. B. (2003). Trends in track forecasting for tropical cyclones threatening the United States, 1970–2001. *Bulletin of the American Meteorological Society*, 84(9), 1197-1204.
- Holland, G. J. (1980). An analytic model of the wind and pressure profiles in hurricanes. *Monthly weather review*, 108(8), 1212-1218.
- Hendricks, E. A., Peng, M. S., Ge, X., & Li, T. (2011). Performance of a dynamic initialization scheme in the Coupled Ocean–Atmosphere Mesoscale Prediction System for Tropical Cyclones (COAMPS-TC). *Weather and Forecasting*, 26(5), 650-663.
- Kepert, J. D. (2009). An Observation Operator for the Variational Assimilation of Vortex Position and Intensity. In *Extended Abstracts of Fifth WMO Symposium on the Assimilation of Observations for Meteorology, Oceanography and Hydrology*(Vol. 106, pp. 1-106).
- Kleist, D. T., K. L. Howard, R. Mahajan, and M. J. Brennan. (2016). Exploring the impact of tropical cyclone relocation for the operational NCEP GFS/GDAS. *96<sup>th</sup> Amer. Meteor. Soc. Conf. on DA and Observing Systems II, New Orleans, LA*.
- Kleist, D. T., & Ide, K. (2015). An OSSE-based evaluation of hybrid variational–ensemble data assimilation for the NCEP GFS. Part I: System description and 3D-hybrid results. *Monthly Weather Review*, 143(2), 433-451.
- Kleist, Daryl T., and Kayo Ide. "An OSSE-based evaluation of hybrid variational–ensemble data assimilation for the NCEP GFS. Part II: 4D-EnVar and hybrid variants." *Monthly Weather Review* 143, no. 2 (2015): 452-470.
- Kurihara, Y., Bender, M. A., & Ross, R. J. (1993). An initialization scheme of hurricane

- models by vortex specification. *Monthly weather review*, 121(7), 2030-2045.
- Kwon, H. J., Won, S. H., Ahn, M. H., Suh, A. S., & Chung, H. S. (2002). GFDL-type typhoon initialization in MM5. *Monthly weather review*, 130(12), 2966-2974.
- Kwon, I. H., & Cheong, H. B. (2010). Tropical cyclone initialization with a spherical high-order filter and an idealized three-dimensional bogus vortex. *Monthly Weather Review*, 138(4), 1344-1367.
- Liu, Q., Marchok, T., Pan, H. L., Bender, M., & Lord, S. (2000). *Improvements in hurricane initialization and forecasting at NCEP with global and regional (GFDL) models*. US Department of Commerce, National Oceanic and Atmospheric Administration, National Weather Service, Office of Meteorology, Science Division.
- Leslie, L. M., & Holland, G. J. (1995). On the bogussing of tropical cyclones in numerical models: A comparison of vortex profiles. *Meteorology and Atmospheric Physics*, 56(1-2), 101-110.
- Marchok, T. P. (2002, April). How the NCEP tropical cyclone tracker works. In *Preprints, 25th Conf. on Hurricanes and Tropical Meteorology, San Diego, CA, Amer. Meteor. Soc. P* (Vol. 1).
- Nehrkorn, T., Woods, B. K., Hoffman, R. N., & Auligné, T. (2015). Correcting for position errors in variational data assimilation. *Monthly Weather Review*, 143(4), 1368-1381.
- Montgomery, M. T., & Smith, R. K. (2014). *Paradigms for tropical cyclone intensification*. NAVAL POSTGRADUATE SCHOOL MONTEREY CA DEPT OF METEOROLOGY.
- Pu, Z. X., & Braun, S. A. (2001). Evaluation of bogus vortex techniques with four-dimensional variational data assimilation. *Monthly weather review*, 129(8), 2023-2039.
- Rappin, E. D., Nolan, D. S., & Majumdar, S. J. (2013). A highly configurable vortex initialization method for tropical cyclones. *Monthly Weather Review*, 141(10), 3556-3575.
- Smith, R. K., Zhang, J. A., & Montgomery, M. T. (2017). The dynamics of intensification in a

Hurricane Weather Research and Forecasting simulation of Hurricane Earl (2010). *Quarterly Journal of the Royal Meteorological Society*, 143(702), 293-308.

Wang, X., & Lei, T. (2014). GSI-based four-dimensional ensemble–variational (4DEnsVar) data assimilation: Formulation and single-resolution experiments with real data for NCEP Global Forecast System. *Monthly Weather Review*, 142(9), 3303-3325.

Wu, C. C., Lien, G. Y., Chen, J. H., & Zhang, F. (2010). Assimilation of tropical cyclone track and structure based on the ensemble Kalman filter (EnKF). *Journal of the Atmospheric Sciences*, 67(12), 3806-3822.

Zhang, B., Lindzen, R. S., Tallapragada, V., Weng, F., Liu, Q., Sippel, J. A., ... & Bender, M. A. (2016). Increasing vertical resolution in US models to improve track forecasts of Hurricane Joaquin with HWRF as an example. *Proceedings of the National Academy of Sciences*, 113(42), 11765-11769.

Zou, X., & Xiao, Q. (2000). Studies on the initialization and simulation of a mature hurricane using a variational bogus data assimilation scheme. *Journal of the atmospheric sciences*, 57(6), 836-860.

## Appendix I The relocation information during the experiment period

TIME	NAME/STATION	Observed		Model Field		DISPLACEMENT (DEGREE)		
		LON	LAT	LON	LAT	LON	LAT	Displacement (degree)
2015/09/28 00	NHC 11L	291.40	27.40	289.80	27.90	1.60	-0.50	1.68
2015/09/28 06	NHC 11L	291.20	27.40	291.00	27.70	0.20	-0.30	0.36
2015/09/28 12	NHC 11L	290.90	27.40	290.80	27.80	0.10	-0.40	0.41
2015/09/28 18	NHC 11L	290.00	27.50	290.40	27.60	-0.40	-0.10	0.41
2015/09/29 00	NHC 11L	289.80	26.80	290.00	27.10	-0.20	-0.30	0.36
2015/09/29 06	JOAQUIN	289.60	26.60	289.70	26.90	-0.10	-0.30	0.32
2015/09/29 12	JOAQUIN	289.40	26.50	289.40	26.60	0.00	-0.10	0.10
2015/09/29 18	JOAQUIN	289.20	26.00	289.00	26.40	0.20	-0.40	0.45
2015/09/30 00	JOAQUIN	288.50	25.80	288.90	26.00	-0.40	-0.20	0.45
2015/09/30 06	JOAQUIN	288.00	25.60	288.30	25.60	-0.30	0.00	0.30
2015/09/30 12	JOAQUIN	287.70	24.80	287.40	25.20	0.30	-0.40	0.50
2015/09/30 18	JOAQUIN	287.10	24.50	287.30	24.70	-0.20	-0.20	0.28
2015/10/01 00	JOAQUIN	287.00	23.90	287.30	24.20	-0.30	-0.30	0.42
2015/10/01 06	JOAQUIN	286.50	23.50	286.60	23.60	-0.10	-0.10	0.14
2015/10/01 12	JOAQUIN	286.30	23.10	286.20	23.40	0.10	-0.30	0.32
2015/10/01 18	JOAQUIN	285.80	23.00	286.00	23.20	-0.20	-0.20	0.28
2015/10/02 00	JOAQUIN	285.60	22.90	285.60	22.90	0.00	0.00	0.00
2015/10/02 06	JOAQUIN	285.30	23.00	285.20	23.20	0.10	-0.20	0.22
2015/10/02 12	JOAQUIN	285.20	23.30	285.20	23.40	0.00	-0.10	0.10
2015/10/02 18	JOAQUIN	285.20	23.80	285.20	23.80	0.00	0.00	0.00
2015/10/03 00	JOAQUIN	285.70	24.30	285.90	24.30	-0.20	0.00	0.20
2015/10/03 06	JOAQUIN	286.30	24.90	286.40	24.90	-0.10	0.00	0.10
2015/10/03 12	JOAQUIN	287.40	25.60	287.50	25.70	-0.10	-0.10	0.14
2015/10/04 00	JOAQUIN	290.50	27.40	290.20	27.40	0.30	0.00	0.30
2015/10/04 06	JOAQUIN	291.80	29.00	291.70	28.80	0.10	0.20	0.22
2015/10/04 12	JOAQUIN	292.90	30.40	292.70	30.30	0.20	0.10	0.22
2015/10/04 18	JOAQUIN	293.40	31.70	293.60	31.90	-0.20	-0.20	0.28
2015/10/05 00	JOAQUIN	294.20	32.60	293.90	32.70	0.30	-0.10	0.32